सत्यं शिवं सुन्दरम्

Chapter-4

Result and Discussion

Feronia limonia

4. *Feronia limonia*

The systematic studies were undertaken on leaves, stem bark and root bark of *Feronia limonia* in order to evolve parameters for standardization and to access their hepatoprotective activity. The results of different studies are compiled and discussed under following headings:

- Pharmacognostic studies and proximate analysis
- Preliminary phytochemical evaluation
- Separation and identification of bioactive marker constituents
- Biological evaluation

4.1 Pharmacognostical studies

Some important pharmacognostical features of various parts of *Feronia limonia* are documented here.

4.1.1 Macroscopic features

Feronia limonia have imparipinnate, unipinnate compound leaves arranged in alternate manner. They are 2.5 - 3 cm long, dark green, obovate with an obtuse notched or cenulate apex. 3-9 leaflets are petiolate and arranged oppositely on a flat-rachis. The leaflets are gland dotted and slightly lemon scented when crushed. Stem bark is ridged, fissured and scaly and there are sharp spines: 3/4 to 2 in (2-5 cm) long on some of the zigzag twigs. Macroscopically the stem bark have dark brown colour on outer surface, sweet odour and rough spiny surface. Root bark have light brown colour on outer surface and yellow colour on inner surface with sweet odour. Photographs of leaves, stem bark and root bark is given in Figure 4.1 and there characteristic features are reported in Table 4.1.

Figure 4.1 Photographs of stem bark, leaves and root bark of *Feronia limonia*

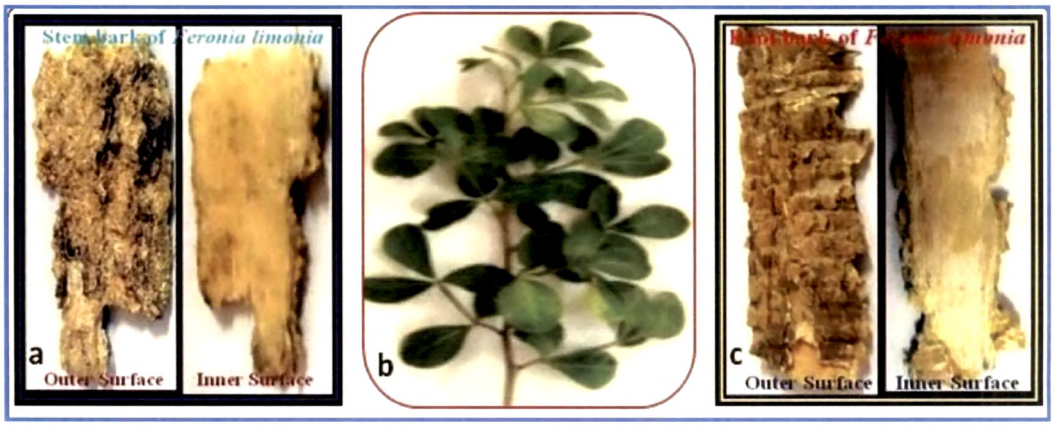

a) Outer and inner surface of stem bark, b) leaves, c) Outer and inner surface of root bark of FL

Table 4.1 Characteristic macroscopic features of leaves stem bark and root bark of *F. limonia*

Features	Observations		
	Leaf	Stem bark	Root bark
Colour			
-Inner surface	Green	Yellow	Light yellow
-Outer surface	Dark green	Dark brown	Light brown
Odour	Lemon-scented	Sweet smell	Sweet smell
Taste	Bitter	Taste less	Taste less
Shape	Ovate to obovate		
Fracture	-	Ridged, fissured	Ridged, Scally
Size			
-Length	7.5 – 12 mm	12-18 cm	10-15 cm
-Breadth	3 – 5 mm	5 mm	3 mm

These features will assist in identifying the selected drug on preliminary basis.

4.1.2 Microscopic studies

Microscopic evaluation of medicinal herb is an indispensible and cost effective tool in the conventional analytical pharmacy for the identification of medicinal herb (Wallis, 1965). Uses of microscopic characteristics have been the main stay of classical Pharmacognosy and remains as one of the essential component of the modern monographs. In this regard, the important microscopic features of the leaves, stem bark and root bark have been documented.

4.1.2.1 Transverse section of leaf

The leaves of *Feronia limonia* are dorsiventral or bifacial with distinct adaxial and abaxial faces. At transection, the midrib appears to be biconvex with the adaxial surface being more convex than abaxial surface.

A transection through the lamina shows an adaxial/ upper epidermis made up of barrel shaped cells covered with a thick cuticle. The abaxial /lower epidermis is made up of rectangular / barrel shaped cells with thick cuticle which distinctly forms on outer and inner ledges on the the guard cells and the subsidiary cells of the stomata. The abaxial epidermis at some location appears multilayered. Below the adaxial epidermis a single row of large hypodermal cells with dense contents appears which extends into the midrib region.

Mesophyll region distinctly differentiated into palisade and spongy tissues. Cells of palisade parenchyma are very compactly arranged in four layers, the length of the cells becoming shorter towards the centre of mesophyll.

The cells of the spongy parenchyma are compactly arranged in strata. The leaves are hypostomatic. Stomata are restricted to the lower epidermis with the guard cells sunken relative to the other epidermal cells. A protuberance of the guard cell wall is present above and below the stomatal aperture. These Protuberances appears as horn shaped ledges.

In the midrib region below one/two layers of hypodermis on the adaxial side, collenchyma is present and above the abaxial epidermis two layers of parenchyma are present. Embedded in the isodiametric ground parenchyma, two collateral bundles are arranged oppositely nearly in the form of a closed arc. The vascular bundles are with several xylem elements arranged in radial rows. Phloem lies towards the epidermises. Conducting elements of phloem is seen alternating with sclerenchyma cells. The microscopic features of TS leaf are depicted in Figure 4.2 and its quantitative details are represented in Table 4.2.

Table 4.2 Quantitative microscopic features of *Feronia limonia* leaves

Sr. No.	Characteristic features		Size (µm)
1	Cuticle Thickness	Lower epidermis	11.10
		Upper epidermis	7.4
2	Upper epidermal layer	Length of cells	14.80
		Width of cells	15.24
3	Lower epidermal layer	Length of cells	14.80
		Width of cells	18.75
4	Hypodermal layer	Length of cells	45.63
		Width of cells	52.17
5	Leaf thickness	Palisade layer	127.85
		Spongy layer	141.71
6	Palisade layer	Length of cells	35.15
		Width of cells	22.57
s7	Spongy layer cells	Length of cells	24.79
		Width of cells	25.9

Figure 4.2 Transverse sections showing various characteristic features of *Feronia limonia* leaves

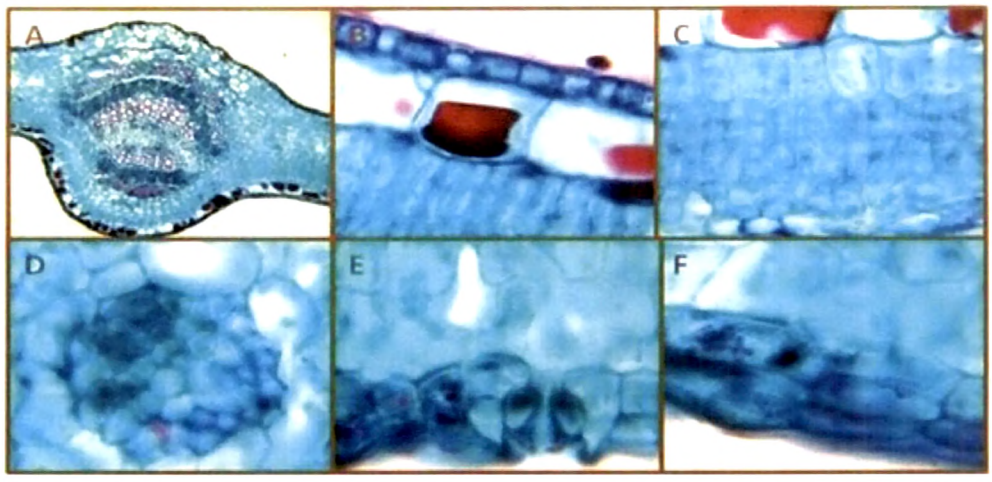

A) Transection through the lamina, B) Adaxial/Upper epidermis with a thick cuticle and hypodermal cells, C) Hypodermal cells with 4 layers of palisade parenchyma, D) Vascular bundle/ lateral veins, E) Stomata with cuteculae ledges, F) Abaxial/lower epidermis

4.1.2.1a Surface preparation of leaf/Micromorphological features:

Both upper and lower epidermises comprises of polygonal cells with straight or slightly arched anticlinal walls. Trichomes are simple, unicellular and with a very thick wall. Each stroma is surrounded by 4-5 subsidiary cells. The leaves are amphistomatic with anisocytic type of stomata on both surfaces. Stomatal index of the lower epidermis is more than the upper epidermis. The microscopic features of the leaf are depicted in Figure 4.3 and its quantitative details are represented in Table 4.3

Table 4.3 Leaf constants of *Feronia limonia*

Leaf constant	Value
Stomatal number	
Upper epidermis	45
Lower epidermis	72
Stomatal index	
Upper epidermis	0.04-0.05
Lower epidermis	5-8
Palisade ratio	31.5
Vein- islet number	2-3
Vein termination number	8-9

Figure 4.3 Transverse section showing stomata of *Feronia limonia* leaf

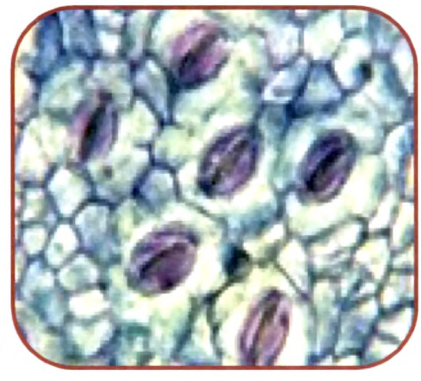

4.1.2.2 Transverse section of stem bark

Stem of *Feronia limonia* appears to comprise of a ring bark. The outermost periderm layers alternate with the darkly stained closing layer. Newly formed periderm/ cork is composed of 25 rows of tangentially elongated, rectangular thin walled cells. The phellogen is 1-2 layered and is not easily distinguishable from the phloem cells. Pheloderm cells are distinctly differentiated from the corticle cells in being radially arranged in rows with the phellogen cells. The corticle cells sub tending the phelloderm cells are elongated and with starch grains. Patches of tangentially elongated stone cells are present between them. These stone cells are arranged parallel placed one above the other.

The outermost region of living/ conducting phloem elements is occupied by bands of sclerenchymatous cells alternating with phloem elements. Cells lying close to sclerenchya show crystals and starch grains. Various characteristic features of TS stem bark shown in Figure 4.4.

Figure 4.4 Transverse sections showing various characteristic features of *F. limonia* stem bark

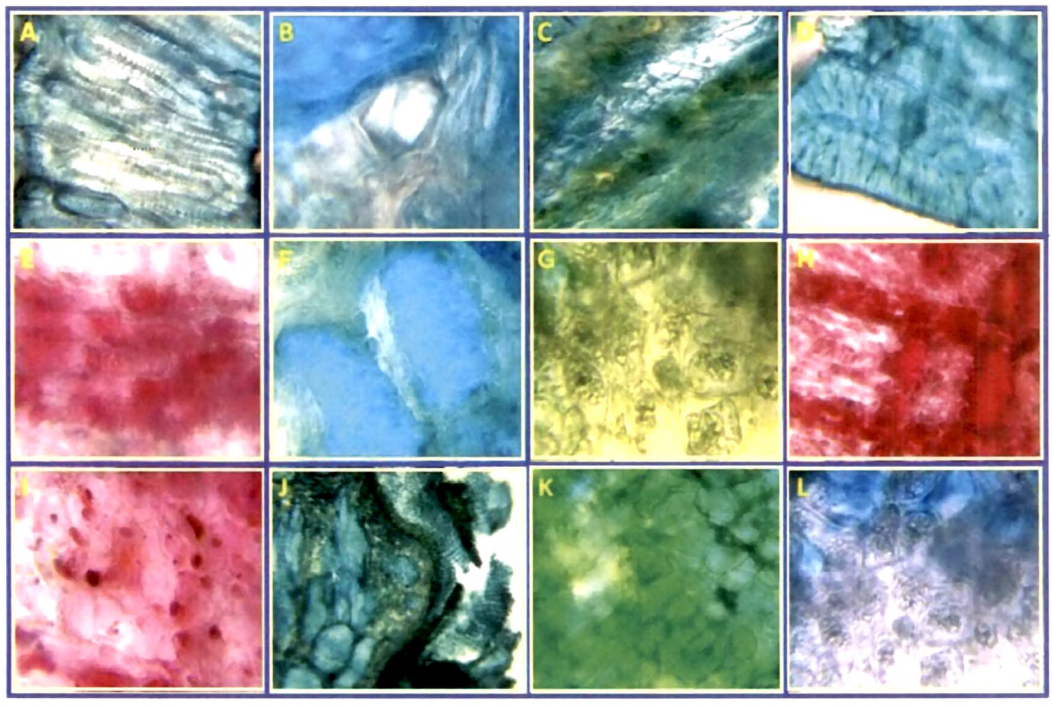

A) Bands of sclerotic cells, B) Rhomboidal crystal,C) D) Enlarged view of sclerotic cell showing pits, E) Cells of phelloderm, F) Sclerotic bands alternating with phloem, G) presence of starch grains, H)Inner bark showing sclerotic bands alternating with phloem, I) phloem elements, J) periderm composed of around 23-25 layers of tangentially elongated cells, K) phloem elements, L) starch grains

4.1.2.3 Transverse section of root bark

The outermost region shows presence of cork layers. The cortex consists of several rows of cells but compressed in appearance. The corticle region consists of large thin walled cells. The outermost phloem cells appear obliterated. The shape of phloem appears to be conical due to the tangential dilation of phloem ray which extends upto the cortex. The corticle cells are large, round and with abundant starch grains. Interspared between the cortical cells patches of sclerenchymatous cells are present which is probably the pericyclic fibres which has with the increase in the diameter of the root become broken down into small patches.

The inner active phloem elements appear to be orderly arranged in radially arranged complexes i.e, arranged in tiers alternating with 4-5 rows of elongated thin walled medullary ray cells. The medullary ray cells show presence of rhomboidal crystals. The numbers of actively periclinally dividing cambial cells appear to be 5-6, arranged in radially rows. Various characteristic features of TS root bark shown in Figure 4.5.

Figure 4.5 Transverse sections showing various characteristic features of *Feronia limonia* root bark

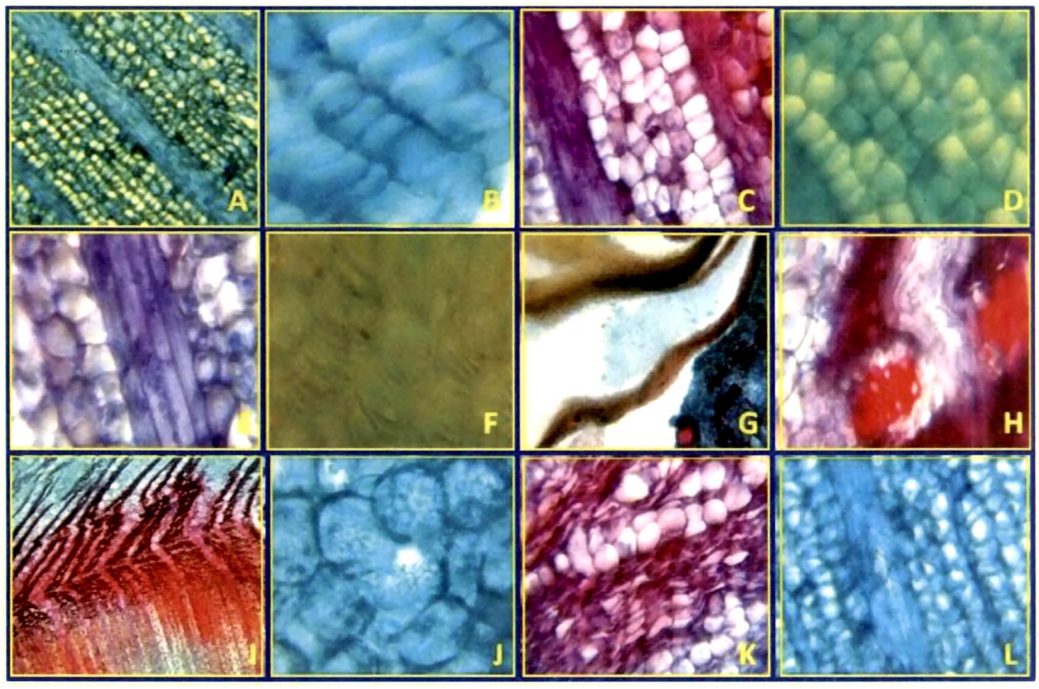

A-phloem region, B)Layers of cambium, C) phloem elements, D) phloem elements, E) Four rows of medullary rays, F) Not clear, G) outermost region of the bark, H, I) outermost region of the bark showing periderm and phloem J) cortical region with starch grains K) Obliterated phloem L) Solitary crystal in medullary ray

4.1.3 Powder microscopic features of Feronia limonia

When the same organ of closely allied taxa forms the source for traditional medicine and substituted with similar organ of other plant, microscopy alone may be inadequate for the purpose of an unequivocal diagnosis. In such case, powder characters are of great value for identifying the powdered crude drugs. The photomicrographs and details of characteristic powder microscopic features of leaves, stem bark and root barks were depicted in Figure 4.6, 4.7 and 4.8.

Figure 4.6 Various powder microscopic features of *Feronia limonia* leaves

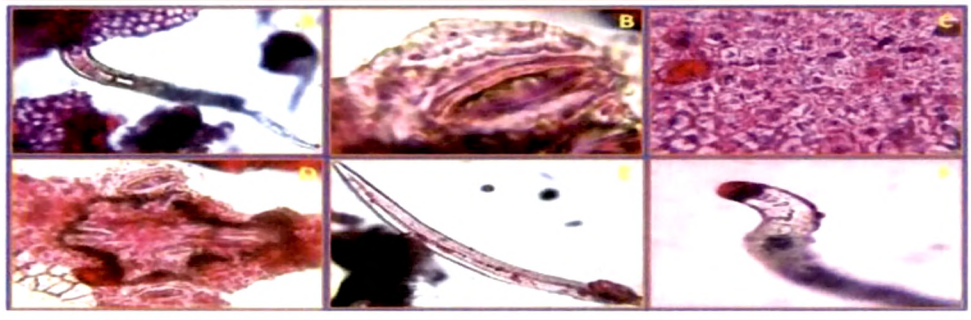

A) Multicellular uniseriate trichome, B) Stomata on leaf fragment, C) Polygonal epidermal cells with straight anticlinal walls, D) epidermis with stomata, E) Unicellular trichome

Figure 4.7 Various powder microscopic features of *F. limonia* stem bark

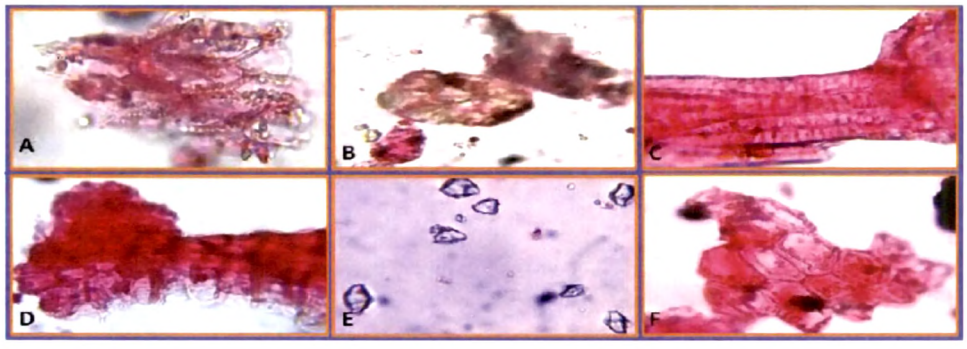

A) *P*helloderm cell B) Periderm cell C) Xylem cells D) Cork cell , E) Rhomboidal crystals, F) Parenchyma cells

Figure 4.8 Various powder microscopic features of *Feronia limonia* root bark

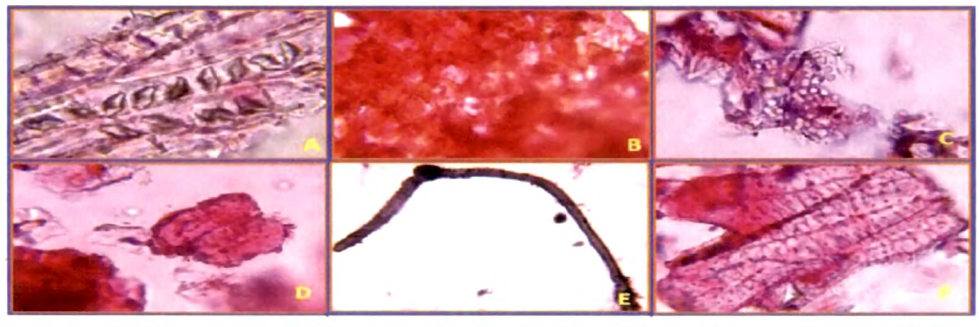

A) Parenchyma with crystals, B) Parenchyma cells, C) Starch grain with parenchyma, D) Fibre, E) Xylem fibre

4.1.4 Proximate analysis

Proximate analysis helps to set up certain standards for dried drugs in order to avoid batch-to-batch variation and to judge their quality and purity. Results of proximate analysis of leaves, stem bark and root bark are shown in Table 4.4

Table 4.4 Physico-chemicals constants of leaves, stem bark and root bark of *Feronia limonia*

Parameters	Values% (w/w) * ±SEM		
	Leaves	Stem bark	Root bark
Total Ash	10.16±0.33	16.83±0.15	14.23±0.029
Acid insoluble ash	4.13±0.08	3.93±0.12	3.06±0.08
Water soluble ash	0.46±0.03	5.33±1.01	4.33±0.145
Water soluble extractive values	9.06±0.34	8.53±0.20	10.5±0.20
Alcohol soluble extractive values	5.43±0.23	12.1±0.32	13.5±0.15
Loss on drying	7.22±0.49	9.5±0.13	11.7±0.23

*** values expressed as mean of three readings**

Total ash value was found to be highest in stem bark followed by root bark and leaves. Similarly water soluble extractive values are higher in root bark followed by leaves and stem bark. These determinations provide an idea regarding the probable content of various inorganic metal ions as well as the nature of the constituents present. More ash value indicates the presence of more inorganic matter.

4.1.4.1 Elemental analysis

All the living organisms require inorganic elements for their growth and survival. Medicinal plant contain considerable amounts of mineral constituents, in particular, the presence of essential elements (Mg,Mn,Zn and many others) is a prerequisite for correct growth and development of plants. Inorganic elements in plants also plays role in the accumulation of secondary metabolites such as alkaloids, glycosides, terpenoids, phenolic compounds etc. (Andrijani, 1998) as their responsible for the activity of a number of enzymatic systems, which in turn regulate the metabolic pathways leading to the synthesis of these compounds. Results of elemental analysis of plant material under study viz., leaves, stem bark and root bark of *Feronia limonia* are given in table 4.5.

Table 4.5 Elemental analysis values of leaf, stem bark and root bark of *Feronia limonia*

Elements	Values in ppm		
	Leaves	Stem bark	Root bark
Potassium	4215.6	2103	2486.1
Sodium	279.18	88.83	191.88
Iron	342.85	705.44	557.97
Magnesium	8.6	8.40	8.32
Zinc	29.05	16.22	10.95
Copper	8.0	6.20	7.0
Mangenese	11.34	10.76	23.29

4.1.4.2 Fluorescence analysis

The colour of the plant extract is mainly due to its chemical composition. The same extract may appear in different colours at different wavelength of light. Kokashi et al., 1958 studied the colour behaviour of different meditional drugs under UV radiations and found that specific colour patterns are obtained at 254 and 366 nm , those colours were characteristic for the particular drug or different parts of same drug. The results of fluorescence analysis of leaves, stem bark and root bark are given in Figure no 4.9, 4.10 and 4.11.

Figure4.9 Fluorescence analysis of the methanolic extract of *Feronia limonia* leaves

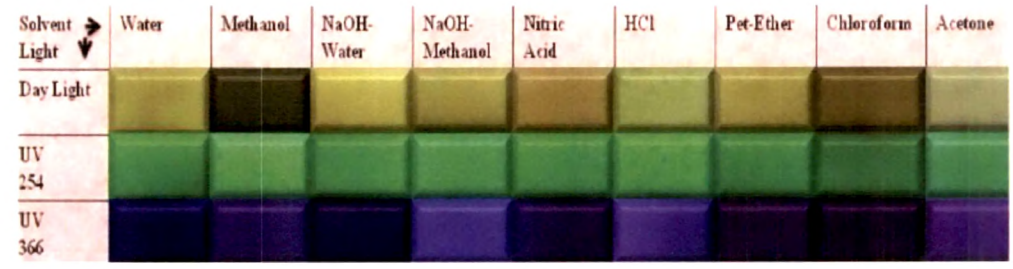

Colour pattern of *Feronia limonia* leaves methanolic extract under ordinary light and UV- 254 and 366 nm with different solvents

Figure 4.10 Fluorescence analysis of the methanolic extract of stem bark

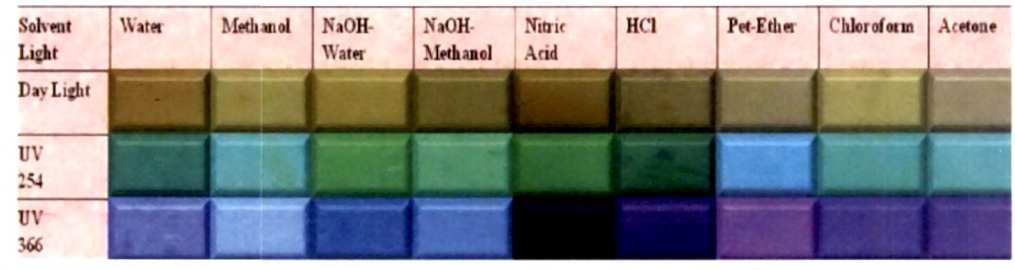

Colour pattern of *Feronia limonia* stem bark methanolic extract under ordinary light and UV-254 and 366 nm with different solvents

Figure 4.11 Fluorescence analysis of the methanolic extract of root bark

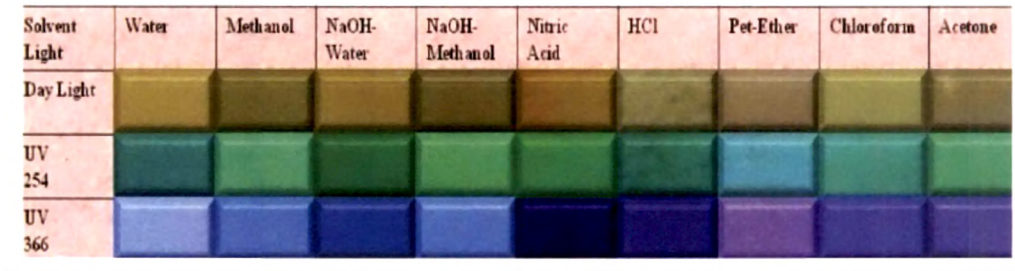

Colour pattern of *Feronia limonia* root bark methanolic extract under ordinary light and UV-254 and 366 nm with different solvents

4.2 Phytochemical analysis of *Feronia limonia*

4.2.1 Successive solvent extraction

The leaves, stem bark and root bark of *Feronia limonia* were separately subjected to successive solvent extraction. Percentage yield of the selected successive extracts were recorded in Table 4.6 .The successive solvent extraction of the drug with solvents of increasing polarity generally results in the separation of the constituents according their polarity. The non polar constituents are extracted in solvents like

petroleum ether, and benzene being non-polar; semi-polar constituents are extracted in chloroform and acetone being semi-polar; while the polar and highly polar constituents are found in ethanol and water. Thus, the values of successive solvent extraction provide an idea regarding the presence of various non-polar, semi-polar and polar constituents.

Leaves of *Feronia limonia* gives maximum extractive value with water, methanol, and petroleum ether, where as with benzene, chloroform and ethyl acetate these extractive values were found to be very less.

Table 4.6 Successive extractive values of the leaves, stem bark and root bark of *Feronia limonia*

Solvent	Values%(w/w)* ±SEM		
	Leaves	Stem bark	Root bark
Petroleum ether	1.90±0.05	1.06±0.02	2.42±0.12
Benzene	0.69±0.02	0.79±0.03	0.46±0.03
Chloroform	0.95±0.02	1.88±0.01	0.65±0.01
Ethyl acetate	0.73±0.06	2.76±0.08	0.31±0.01
Methanol	4.63±0.17	6.26±0.12	4.66±0.12
Water/Aqueous	9.53±0.17	1.70±0.05	2.13±0.14

*** values expressed as mean of three readings**

4.2.2 Phytochemical analysis of successive extracts

Wide variety of natural compounds like alkaloids, glycosides, saponins, phytosterols, phenolics, terpenoids, flavanoids, coumarins and tannins which exert physiological activity are synthesized in plants. In addition to carbohydrates, proteins and lipids which are utilized by man as food. A systematic and complete study of crude drugs by different qualitative chemical tests will provide information regarding the presence and absence of both primary and secondary metabolites derived as a result of plant metabolism. In order to identify the nature and composition of various extracts obtained from successive extraction process were subjected to various qualitative chemical tests to determine the presence of various constituents. Results of phytochemical analysis on various successive extracts are summarized in Table 4.7

Table 4.7 Preliminary phytochemical investigation of *Feronia limonia* leaves, stem bark androot bark

Phytochemical	Pet. Ether Extract			Chloroform Extract			Methanol Extract			Water Extract		
	L	S	R	L	S	R	L	S	R	L	S	R
Alkaloids	–	–	–	–	–	+	–	+	+	–	–	–
Sugars	–	–	–	–	–	–	–	–	–	+	+	+
Phenols	–	–	–	+	+	–	+	+	+	+	+	+
Flavonoids	+	–	–	+	–	+	+	+	+	+	+	+
Saponins	–	–	–	–	–	–	+	+	+	+	–	–
Steroids	+	–	–	+	+	–	+	–	+	–	–	+
Tannins	–	–	–	–	–	–	+	+	+	+	+	+
Coumarins	+	+	+	+	+	+	+	+	+	+	+	+
Terpenoids	+	–	–	+	–	–	–	+	+	–	+	–
Glycosides	–	–	–	–	–	–	–	–	+	+	+	+

'L' Leaves; 'S' Stem bark; 'R' root bark; '+' presence; '-' absence

4.2.3 Total Phenolic, flavanoid and flavanol content of Feronia limonia

The total Phenolic, flavanoid and flavanol content of various parts of *Feronia limonia* viz. leaves, stem bark and root bark in aqueous and methanol extract is given in Table no 4.8

The phenolic content of methanolic and aqueous extract of *Feronia limonia* leaves, stem bark and root bark were found to be 0.0312±0.81and 0.0495±0.75; 0.043±0.70 and 0.0253±1.00; 0.0363±0.80and 0.030±0.49 % w/w respectively, representing the various phenolic compounds like poly phenol, phenolic acid etc.

The flavanoidal content of methanolic and aqueous extract of F. limonia leaves, stem bark and root bark were found to be 0.0015±0.33 and 0.0008±0.12; 0.016±0.13 and 0.005±0.33; 0.012±0.81 and 0.001±0.08 % w/w respectively.

The flavanol content of methanolic and aqueous extract of F. limonia leaves, stem bark and root bark were found to be 0.0011±0.66 and 0.0017±0.63; 0.0144±0.81 and 0.0064±0.33; 0.0021±0.16 and 0.0090±0.66 % w/w respectively.

From the calibration curve of the quercetin, the concentrations of the flavanoids and flavonols in the methanol extract and aqueous extract of leaves, stem bark and roots were determined and the results are represented in Table no 4.8.

Table 4.8 Quantitative evaluation of total phenolic, flavanoid and flavanol content of *Feronia limonia* leaves

Plant Parts	Extract	Total[a] Phenolics	Total flavanoids [b] ($AlCl_3$) method	Total[b] Flavanols
Leaves	Methanol	0.0312±0.81	0.0015±0.33	0.0011±0.66
	Aqueous	0.0253±1.00	0.0008±0.12	0.0017±0.63
Stem bark	Methanol	0.0495±0.75	0.016±0.13	0.0144±0.81
	Aqueous	0.0363±0.80	0.005±0.33	0.0064±0.33
Root bark	Methanol	0.043±0.70	0.012±0.81	0.0021±0.16
	Aqueous	0.030±0.49	0.001±0.08	0.0090±0.66

a= mg gallic acid/g; b= mg quercetin/g; * values expressed as mean of three readings; SEM

4.2.4 TLC of the extracts obtained in successive extraction

TLC is a very effective technique for the separation of chemical constituents of extracts and for their identification. Components are separated by the differential migration of solute between two phases - a stationary phase and a mobile phase. Depending on the particular type of stationary phase and using different solvents, separation can be achieved on the basis of partition or a combination of partition and adsorption. Selection of mobile phase is based on the increasing order to polarity and the chemical tests.

Thus, in continuation of our studies on qualitative analysis of secondary metabolites present in successive extracts of leaves, stem bark and root bark *Feronia limonia*, TLC study was carried out on silica gel aluminium plate 60F-254, 0.5 mm. The solvent system used for TLC was hexane/chloroform/methanol (1:4.75:0.25). Phytochemical analysis using HPTLC assays provided qualitative insights into the bioactive constituents of the leaves stem bark and root bark. TLC characterizations of all the successive extracts, showed many spots with different R_f values. Detection was done at UV 254, 366 and 540 nm because secondary metabolites like flavanoids, coumarins, polyphenols etc. gave fluorescence at this nm. The documentation of leaves; stem bark and root bark TLC were shown in figure 4.12, 4.13, 4.14; 4.15, 4.16, 4.17 and 4.18, 4.19, 4.20.

4.2.4.1 TLC fingerprinting of successive extracts of Feronia limonia leaves

Figure 4.12 TLC of the extracts obtained from leaves in successive extraction at 254 nm

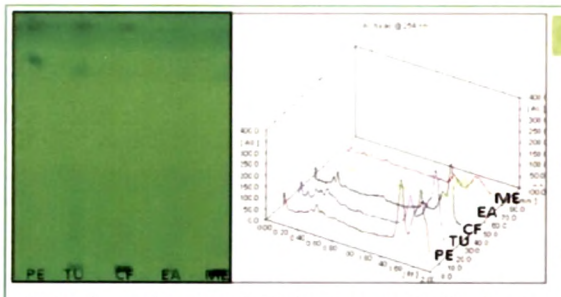

S.N.	N. of Peak	RF
PE	5	0.06, 0.39, 0.45, 0.50
TU	10	0.07, 0.15, 0.26, 0.31, 0.40, 0.48, 0.60, 0.77
CL	9	0.06, 0.28, 0.33, 0.81, 0.88,
EA	4	0.26, 0.32, 0.77
ME	7	0.11, 0.27, 0.35, 0.53, 0.81, 0.88

PE: Petroleum ether extract; TU:T oluene extract; CF: Chloroform extract; EA: Ethyl acetate extract; ME: Methanol extract

TLC profile, three dimensional overlaid spectrum and qualitative details of chemical constituents present in successive extract of *Feronia limonia* leaves at 254 nm

Figure 4.13 TLC of the extracts obtained from leaves in successive extraction at 366 nm

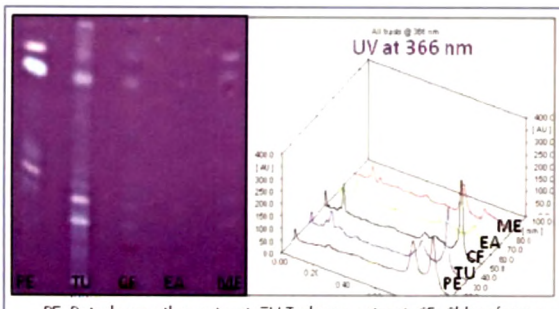

S.N.	N.of Peak	RF
PE	4	0.01, 0.22, 0.76, 0.88
TU	7	0.01, 0.11, 0.14, 0.21, 0.30, 0.71, 0.88
CL	5	0.01, 0.12, 0.64, 0.71, 0.87
EA	5	0.02, 0.11, 0.67, 0.84, 0.87
ME	5	0.12, 0.16, 0.46, 0.69, 0.83

PE: Petroleum ether extract; TU:T oluene extract; CF: Chloroform extract; EA: Ethyl acetate extract; ME: Methano extract

TLC profile, three dimensional overlaid spectrum and qualitative details of chemical constituents present in successive extract of *Feronia limonia* leaves at 366 nm

Figure 4.14 TLC of the extracts obtained from leaves in successive extraction at 540 nm

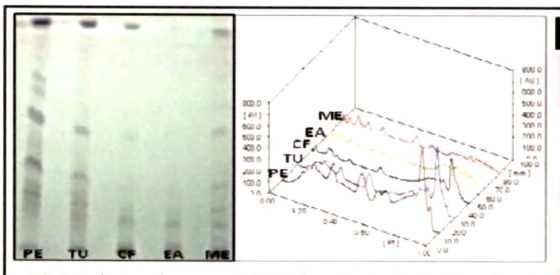

PE: Petroleum ether extract; TU:T oluene extract; CF: Chloroform extract; EA: Ethyl acetate extract; ME: Methanol extract

S.N.	N. of Peak	RF
PE	13	0.14, 0.16, 0.20, 0.23, 0.32, 0.38, 0.51, 0.61, 0.66, 0.80, 0.84, 0.90, 0.94
TU	11	0.12, 0.14, 0.17, 0.28, 0.46, 0.56, 0.62, 0.78, 0.83, 0.89, 0.95
CL	10	0.02, 0.11, 0.16, 0.24, 0.44, 0.77, 0.80, 0.83, 0.88, 0.96
EA	10	0.02, 0.10, 0.15, 0.76, 0.80, 0.82, 0.85, 0.89, 0.93, 0.96
ME	12	0.01, 0.05, 0.10, 0.17, 0.26, 0.47, 0.57, 0.63, 0.70, 0.76, 0.82, 0.85

TLC profile, three dimensional overlaid spectrum and qualitative details of chemical constituents present in successive extract of *Feronia limonia* leaves at 540 nm after derivatization with AS

4.2.4.2 TLC fingerprinting of successive extracts of Feronia limonia stem bark

Figure 4.15 TLC of the extracts obtained from stem bark in successive extraction at 254 nm

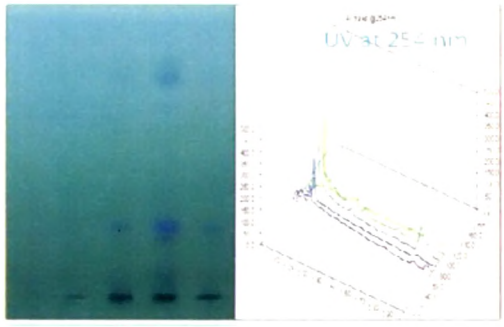

Sample	N. of peaks	Rf
PE	5	0.06,0.15,0.23,0.88,0.97
TU	4	0.06,0.14,0.30,0.87
CL	8	0.06,0.014,0.21,0.23,0.34,0.38, 0.87,0.91
EA	11	0.05,0.19,0.21,0.24,0.33,0.38, 0.46,0.68,0.76,0.88,0.91
ME	7	0.05,0.13,0.20,0.32,0.37,0.86, 0.90

TLC profile, three dimensional overlaid spectrum and qualitative details of chemical constituents present in successive extract of *Feronia limonia* stem barks at 254 nm

Figure 4.16 TLC of the extracts obtained From stem bark in successive extraction at 366 nm

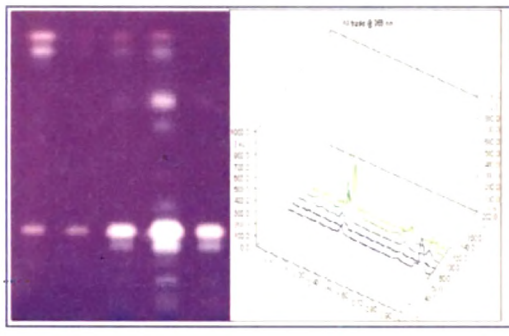

Sample	N. of peaks	Rf
PE	7	0.12,0.32,0.38,0.68,0.82,0.88, 0.97
TU	6	0.12,0.22,0.38,0.72,0.88,0.97
CL	8	0.12,0.32,0.38,0.58,0.64,0.72, 0.87,0.97
EA	10	0.09,0.12,0.17,0.32,0.48,0.62, 0.68,0.82,0.88,0.97
ME	7	0.09,0.12,0.17,0.38,0.58,0.82, 0.88

LC profile, three dimensional overlaid spectrum and qualitative details of chemical constituents present in successive extract of *Feronia limonia* stem barks at 366 nm

Figure 4.17 TLC of the extracts obtained from stem bark in successive extraction at 540 nm

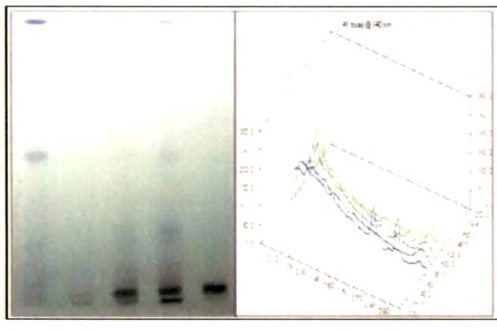

Sample	N. of peaks	Rf
PE	9	0.08,0.14,0.19,0.24,0.32,0.45,0.62, 0.79,0.95
TU	6	0.07,0.13,0.15,0.24,0.46,0.94
CL	7	0.09,0.13,0.16,0.33,0.61,0.73,0.91
EA	9	0.12,0.16,0.23,0.32,0.35,0.42,0.61, 0.78,0.84,
ME	6	0.09,0.12,0.16,0.22,0.30,0.94

TLC profile, three dimensional overlaid spectrum and qualitative details of chemical constituents present in successive extract of *Feronia limonia* stem barks at 540 nm after derivatization with AS

4.2.4.3 TLC fingerprinting of successive extracts of Feronia limonia root bark

Figure 4.18 TLC of the extracts obtained from root bark in successive extraction at 254 nm

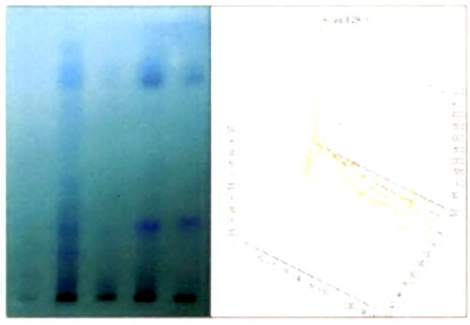

Sample	N. of peaks	Rf
PE	7	0.04,0.13,0.18,0.20,0.24,0.32,0.86
TU	11	0.04,0.13,0.18,0.28,0.36,0.44,0.52, 0.65,0.76,0.86,0.90
CL	8	0.01,0.08,0.13,0.27,0.36,0.66,0.81, 0.97
EA	8	0.12,0.33,0.37,0.46,0.76,0.86,0.90, 0.98
ME	9	0.09,0.12,0.18,0.21,0.28,0.35,0.38, 0.48,0.87

TLC profile, three dimensional overlaid spectrum and qualitative details of chemical constituents present in successive extract of *Feronia limonia* root barks at 254 nm

Figure 4.19 TLC of the extracts obtained from root bark in successive extraction at 366 nm

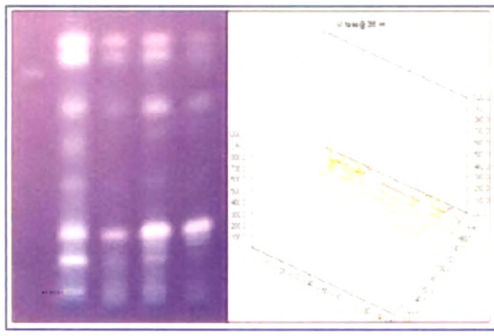

Sample	N. of peaks	Rf
PE	2	0.13, 0.80
TU	10	0.10, 0.21, 0.28, 0.32, 0.37, 0.46, 0.52, 0.64, 0.76, 0.92
CL	6	0.18, 0.27, 0.36, 0.75, 0.92, 0.97
EA	10	0.13, 0.16, 0.19, 0.28, 0.33, 0.37, 0.68, 0.76, 0.92, 0.97
ME	6	0.13, 0.18, 0.35, 0.39, 0.77, 0.93

TLC profile, three dimensional overlaid spectrum and qualitative details of chemical constituents present in successive extract of *Feronia limonia* root barks at 366 nm

Figure 4.20 TLC of the extracts obtained from root bark in successive extraction at 540 nm

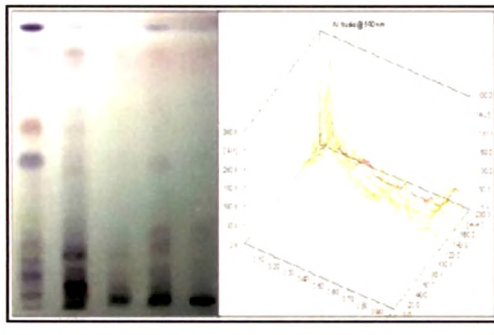

Sample	N. of peaks	Rf
PE	13	0.07,0.12,0.16,0.22,0.27,0.32,0.37, 0.42,0.53,0.61,0.72,0.92
TU	11	0.06,0.11,0.15,0.18,0.23,0.28,0.35, 0.40,0.56,0.71,0.77
CL	7	0.13,0.160.22,0.28,0.30,0.34,0.56
EA	9	0.08,0.11,0.16,0.23,0.29,0.31,0.35, 0.58,0.77
ME	7	0.11,0.16,0.25,0.33,0.36,0.61,0.78

TLC profile, three dimensional overlaid spectrum and qualitative details of chemical constituents present in successive extract of *Feronia limonia* stem barks at 540 nm after derivatization with AS

4.2.5 Qualitative HPLC fingerprinting of Feronia limonia

Standardization and characterization of herbal drugs is a topic of continuous scientific interest in the herbal drug industry. With the advent of modern chromatographic systems there is an ever increasing intent to produce and develop easy, rapid, convenient and cost effective methods for standardization (Selvamani et al., 2009). For standardization of methanolic extract of FL leaves, stem bark and root bark HPLC is a sensitive and accurate tool that fulfils the above mentioned requirements and is widely used tool for the quality assessment of plant extract and its derived product/formulation.

4.2.5.1 Qualitative HPLC fingerprinting of Feronia limonia leaves

Results of HPLC analysis of FL methanolic extract (mobile phase, methanol-water; 1:1, flow rate; 2ml/min, detection; 254 nm) shows that various constituents are present in it which is confirmed by the various peaks present in the chromatogram at different retention time (in mins) such as 4.200, 4.467, 4.790, 5.283, 7.517, 8.493, 10.510, 16.007, 19.287, 25.377, 27.673, 33.070 and 35.420 (Figure 4.21). Similarly, at 366 nm the FL methanolic extract shows various peaks at retention time (in mins) 4.217, 4.617, 7.550, 8.563 and 15.983(Figure 4.22) mins.

Figure 4.21 HPLC chromatogram of *Feronia limonia* leaves (methanolic extract) at 254 nm

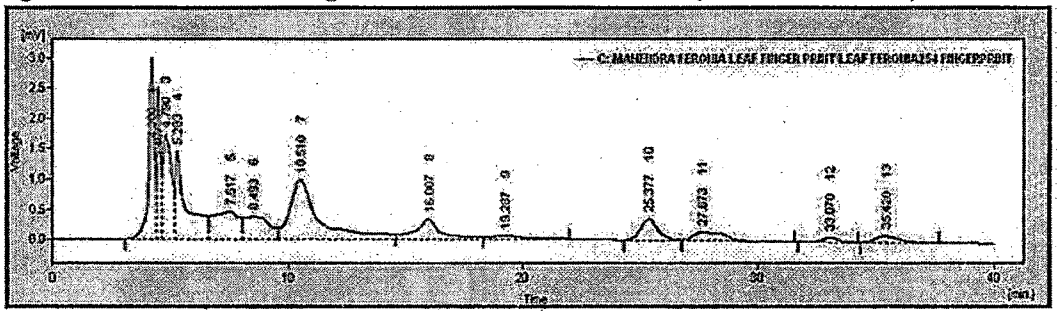

HPLC analysis of leaves methanolic extract (mobile phase, Acetonitrile-water; 75: 25, flow rate; 1ml/min, detection; UV at 254 nm)

Figure 4.22 HPLC chromatogram of *Feronia limonia* leaves (methanolic extract) at 366 nm

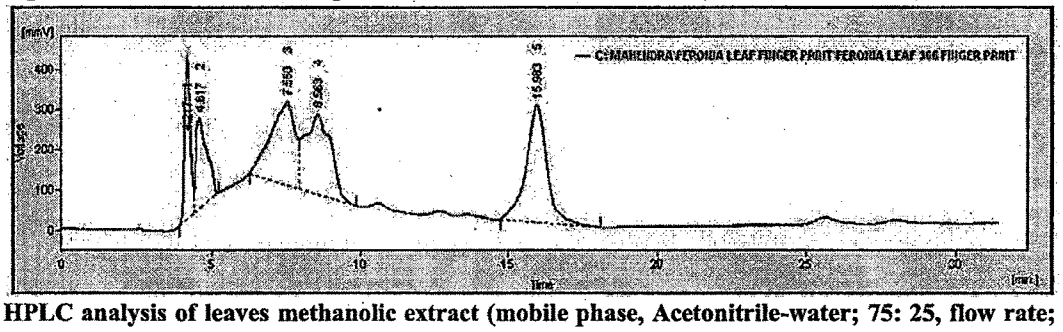

HPLC analysis of leaves methanolic extract (mobile phase, Acetonitrile-water; 75: 25, flow rate; 1ml/min, detection; UV at 366 nm)

4.2.5.2 Qualitative HPLC fingerprinting of Feronia limonia stem bark

Results of HPLC analysis of FL stem bark methanolic extract (mobile phase, methanol-water; 1:1, flow rate; 2ml/min, detection; 254 nm) shows that various constituents are present in it which is confirmed by the various peaks present in the chromatogram at different retention time (in mins) such as 4.023, 4.687, 5.300, 7.443, 10.233, 13.657, 14.637, 15.663, 24.867, 28.013 and 34.643 (Figure 4.23). Similarly, at 366 nm the stem bark methanolic extract shows various peaks at retention time (in mins) 4.017, 4.127, 4.643 and 15.840 (Figure 4.24) mins.

Figure 4.23 HPLC chromatogram of *Feronia limonia* stem bark (methanolic extract) at 254 nm

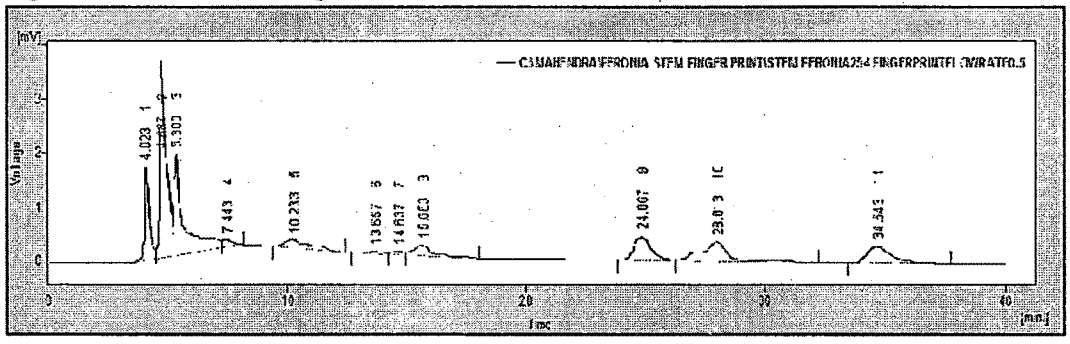

HPLC analysis of stem bark methanolic extract (mobile phase, Acetonitrile-water; 75: 25, flow rate; 1ml/min, detection; UV at 254 nm)

Figure 4.24 HPLC chromatogram of *Feronia limonia* stem bark (methanolic extract) at 366 nm

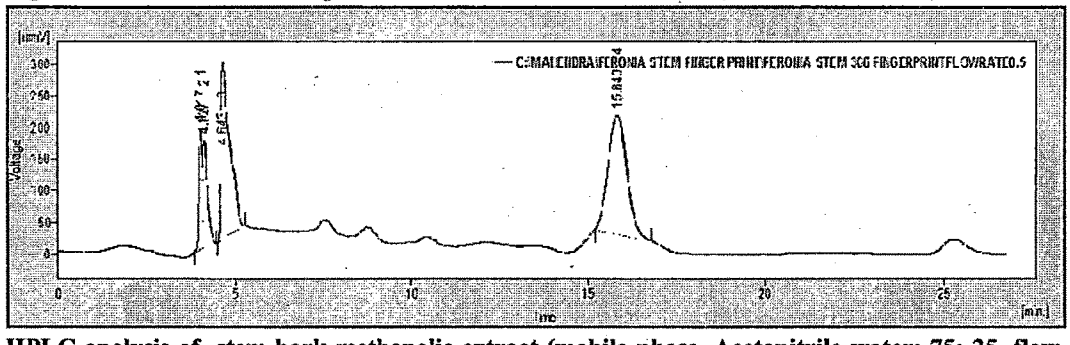

HPLC analysis of stem bark methanolic extract (mobile phase, Acetonitrile-water; 75: 25, flow rate; 1ml/min, detection; UV at 366 nm)

4.2.5.3 *Qualitative HPLC fingerprinting of FL root bark*

Results of HPLC analysis of FL root bark methanolic extract (mobile phase, methanol-water; 1:1, flow rate; 2ml/min, detection; 254 nm) shows that various constituents are present in it which is confirmed by the various peaks present in the chromatogram at different retention time (in mins) such as 3.950, 4.640, 5.297, 10.270, 11.383, 13.623, 15.640, 24.763, 27.047, 32.810, and 34.710 (Figure 4.25). Similarly, at 366 nm the FL methanolic extract shows various peaks at retention time

(in mins) 3.957, 4.557, 4.683, 7.600, 10.503, 13.510, 15.777, 24.967 and 27.230 mins (Figure 4.26).

Figure 4.25 HPLC chromatogram of *Feronia limonia* root bark (methanolic extract) at 254 nm

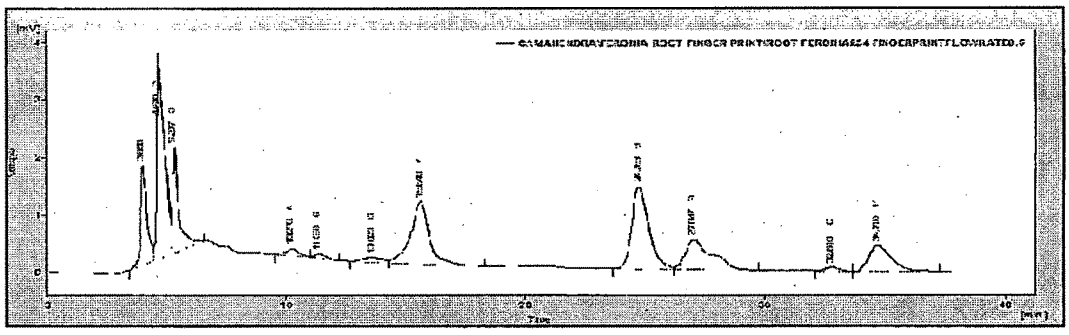

HPLC analysis of stem bark methanolic extract (mobile phase, Acetonitrile-water; 75: 25, flow rate; 1ml/min, detection; UV at 254 nm)

Figure 4.26 HPLC chromatogram of *Feronia limonia* stem bark (methanolic extract) at 366 nm

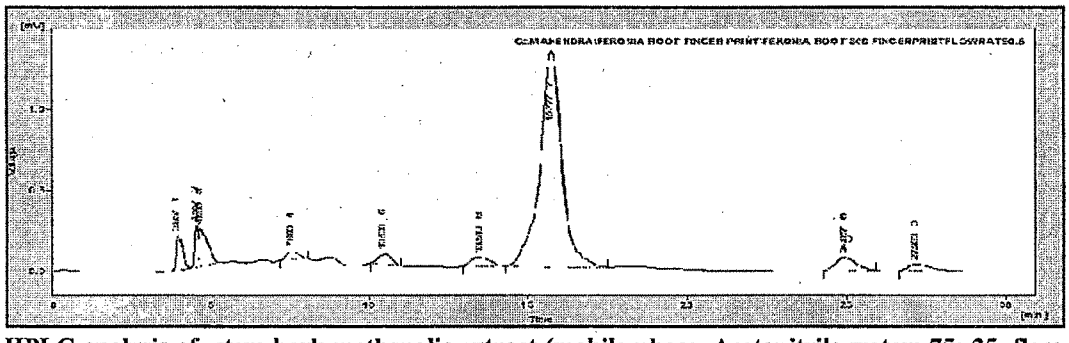

HPLC analysis of stem bark methanolic extract (mobile phase, Acetonitrile-water; 75: 25, flow rate; 1ml/min, detection; UV at 366 nm)

4.3 Phytochemistry of *Feronia limonia*

4.3.1.a Extraction, fractionation and isolation of compound from Feronia limonia leaves

The leaves were shade dried, powdered (500g) and extracted three times with petroleum ether (3X1.5 L) in a soxhlet apparatus. The filtrates were then combined and filtered and concentrated to dryness in a rotary evaporator (Buchi-R-215, Germany) to obtain a crude petroleum ether extract (FL-1). The remaining marc was then dried and again exhaustively extracted at temperature (60-80°C) with methanol (3 × 1.5 L) in a soxhlet apparatus. The pooled extracts obtained were then concentrated under vacuum to give methanolic extract (FL-7). This extract was re-dissolved in water: methanol and partitioned with organic solvents to provide a $CHCl_3$ fraction (FL-9). This fraction was further fractionated by column chromatography

using silica gel (60 # 120 mesh) and eluted with chloroform (100%). A total of 22 test tube fractions were collected. Fractions No. 13, 14 were combined (due to their identical TLC characteristics) to obtained a single fraction (FL-10). This fraction was washed with n-hexane FL-11 to obtain its insoluble portion was purified with preparative TLC using mobile phase toluene-ethyl acetate (9:1) to yield a pure compound MR-2. The % purity of MR-2 was confirmed by analytical HPLC.

Figure 4.27 Graphical representation of MR-2 isolation from *Feronia limonia* leaves

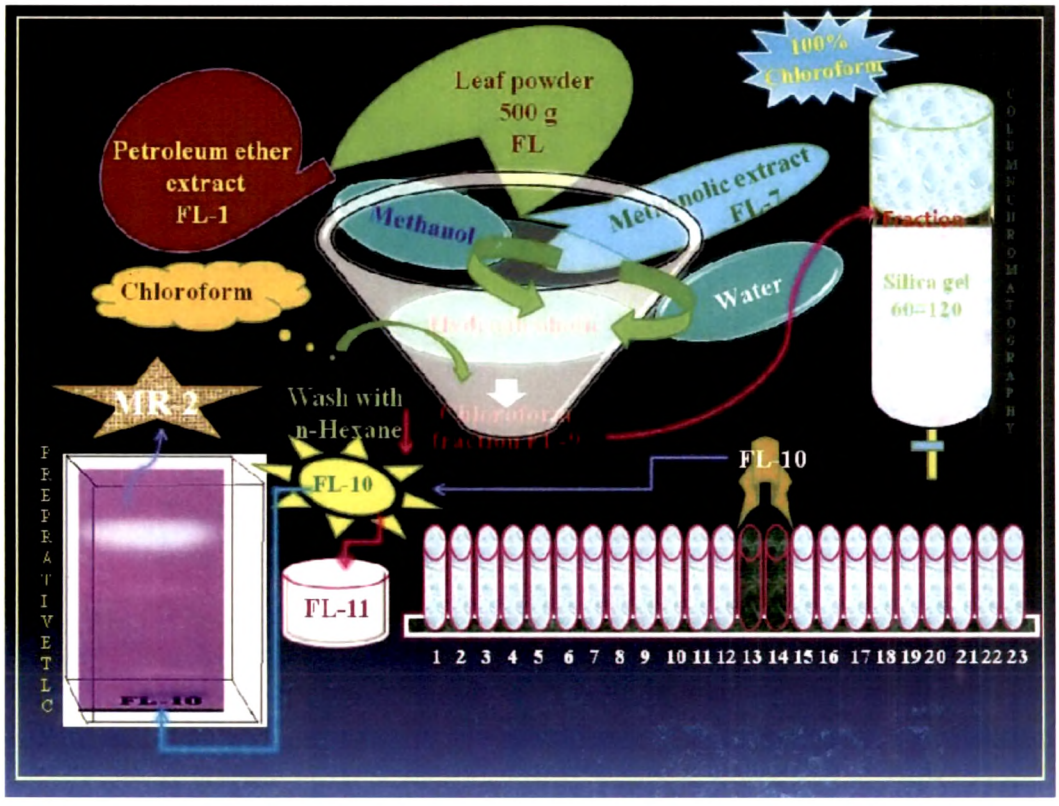

4.3.1.b Extraction, fractionation and isolation of compound from stem bark of Feronia limonia

The stem barks were shade dried, powdered (500g) and extracted three times with petroleum ether (3X1.5 L) in a soxhlet apparatus. The filtrates were then combined and filtered and concentrated to dryness in a rotary evaporator (Buchi-R-215, Germany) to obtain a crude petroleum ether extract (FSB-1). The remaining marc was then dried and exhaustively extracted at 60-80°C with methanol (3 × 1.5 L) in a soxhlet apparatus. The pooled extracts were then concentrated under vacuum to obtain methanolic extract (FSB-7). Hydroalcoholic methanolic extract was made by addition of hot distilled water in methanol (1:1) and partitioned with chloroform (100 mL × 4)

and combined chloroform fraction was then concentrated in vacuum to obtain a brown residue (4.5 g) (FSB-9). This residue was chromatographed over a Silica gel (60#120 mesh size) column eluted with toluene followed by ascending concentrations of ethyl acetate and methanol. The resultant 7th fraction obtained from ethyl acetate-toluene (40:60) yielded an amorphous yellow powder on drying (FSB -11). This powder was subjected to preparative TLC (toluene- ethyl acetate; 85:15) to obtain a pure compound (MR-2). The subsequent 10th fraction obtained from ethyl acetate – toluene (60:40) yielded yellow crystalline fraction (FSB-13) that was further subjected to preparative TLC (chloroform : methanol; 98:2) so as to obtain a pure compound (MR-1), which is characterised by using various spectroscopic techniques viz. Mass, IR, 1H NMR and CHN analysis. Purity of MR-1 and MR-2 compound obtained herein was confirmed by analytical HPLC

Figure 4.28 Graphical representations of MR-1 and MR-2 isolation from *Feronia limonia* stem bark

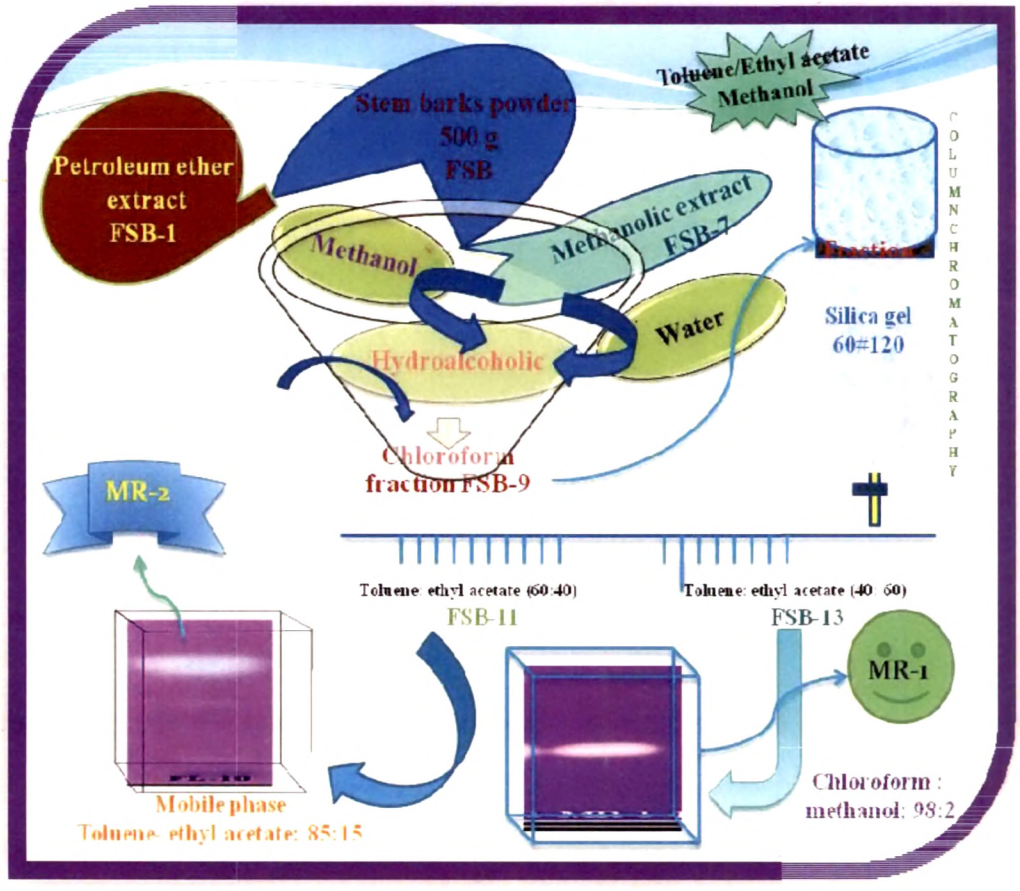

4.3.1.c Extraction, fractionation and isolation of compound from root bark of Feronia limonia

The root bark was shade dried powdered (400 g) and extracted three times with petroleum ether (3×1.5 L) in a soxhlet apparatus. The filtrates were then combined and filtered and concentrated to dryness in a rotary evaporator (Buchi-R-215, Germany) to obtain a crude petroleum ether extract (FRB-1). The remaining marc was then dried and exhaustively extracted at 60-80°C with methanol (3 × 1.5 L) in a soxhlet apparatus. The pooled extracts obtained were then concentrated under vacuum to obtain methanolic extract (FRB-7). Hydro-methanolic extract was made by addition of hot distilled water in methanol (1:1) ratio partitioned with chloroform (100 mL × 4). A combined chloroform fraction was concentrated in vacuum to afford a brown residue (6.2 g) (FRB-9). This residue was blended with silica gel and directly subjected to chromatography on a silica column (60#120 mesh size), eluted with gradient mixture of chloroform: methanol (98: 2v/v), to yield twenty four fractions. The seventh and eighth fractions were mixed because of their identical chromatographic patterns to obtain FRB-10. This was subjected to preparative TLC using toluene: ethyl acetate (85:15) to obtain a pure compound marmesin (MR-1) which was characterised using various spectroscopic techniques viz. Mass, IR, 1H NMR and CHN analysis.

Figure 4.29 Graphical representation of MR-1 isolation from *Feronia limonia* roots bark

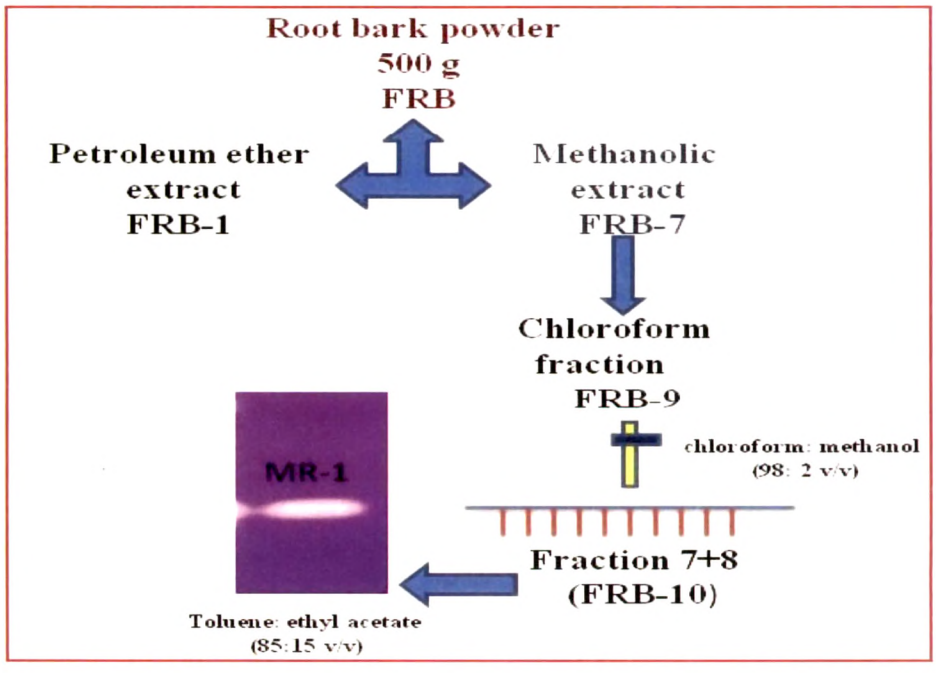

4.3.2 TLC fingerprinting of extracts, fractions and isolated compound from *Feronia limonia*

4.3.2.a Qualitative TLC fingerprinting of leaves

Phytochemical analysis using HPTLC assays provided qualitative insights into the bioactive constituents of the FL-1, FL-7, FL-9, and FL-10 and isolated compound MR-2. TLC characterizations of all the extracts, fractions and isolated compound was done at UV 360 nm because some secondary metabolites like flavanoids, coumarins etc give fluorescence at 360 nm. The chromatogram of extracts and fractions showed many spots with different R_f values such as FL-1, 0.04, 0.16, 0.19, 0.22, 0.27, 0.36, 0.40, 0.48, 0.57, 0.65, 0.67, 0.79, 0.86, 0.89, 0.94; FL-7, 0.03, 0.16, 0.36, 0.48, 0.60, 0.67, 0.78, 0.84; FL-9, 0.03, 0.15, 0.24, 0.44, 0.56, 0.60, 0.66, 0.72, 0.77, 0.84, 0.92; Fl-10, 0.33, 0.60 and chromatogram of isolated compound showed single spot at R_f 0.60. Among the several spots present in FL-7, FL-9, FL-10 one spot exactly matched with the isolated compounds R_f value, and it was found to be more intense compared to the other spots. Hence, it indicated the extract or fractions contain isolated compound. TLC chromatogram of extracts, fractions and isolated compound is shown in figure 4.30.

4.3.2.b Qualitative TLC fingerprinting of stem bark

Qualitative fingerprinting of FSB-1, FSB-7, FSB-9, FSB-11, FSB-13 and isolated compounds MR-1, MR-2 were performed by TLC. A Camag TLC system equipped with Camag Linomat V an automatic TLC sample spotter, Camag glass twin trough chamber (20 × 10 cm), Camag scanner 3 and integrated win CATS 4 Software were used. Pre-coated TLC plate silica gel $60F_{254}$ plates (Kieselgel60F254, Merck, Germany) (Murthy and Mishra, 2008) were used with hexane- chloroform- methanol (1: 4.75: 0.25) for detection of chemical constituent (under UV at 366 nm). TLC chromatogram of extracts, fractions and isolated compound is shown in figure 4.31.

4.3.2.c Qualitative TLC fingerprinting of root bark

Qualitative fingerprinting of FRB-1, FRB-7, FRB-9, FRB-10 and isolated compounds MR-1 were performed by TLC. A Camag TLC system equipped with Camag Linomat V an automatic TLC sample spotter, Camag glass twin trough chamber (20 × 10 cm), Camag scanner 3 and integrated win CATS 4 Software were used. Pre-coated TLC plate silica gel $60F_{254}$ plates (Kieselgel60F254, Merck, Germany) (Murthy and Mishra, 2008) were used with hexane- chloroform- methanol (1: 4.75: 0.25) for

detection of chemical constituent (under UV at 366 nm). TLC chromatogram of extracts, fractions and isolated compound is shown in figure 4.32.

Figure 4.30 TLC fingerprinting and three-dimensional overlaid chromatogram of extracts, fractions and isolated compound from *Feronia limonia* leaf at UV 366 nm.

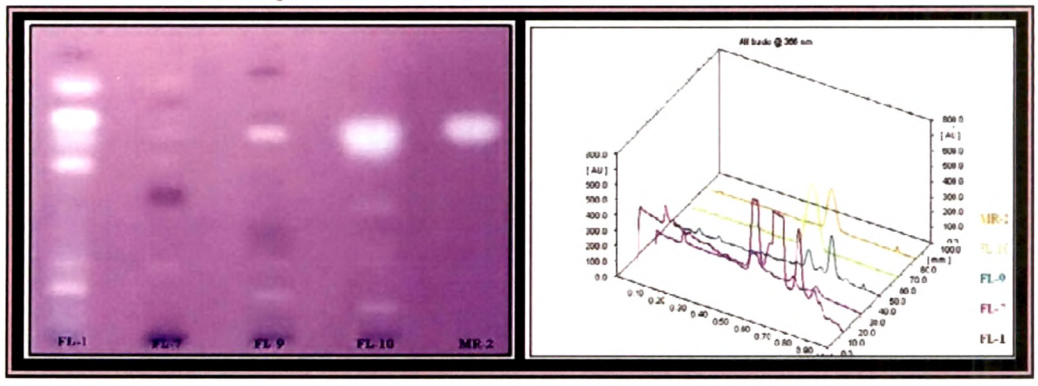

HPTLC analysis of FL-1, FL-7, FL-9, FL-10 and MR-2 (mobile phase, Toluene-ethyl acetate; 85: 15, Linomat V automatic applicator, detection; UV at 365 nm)

Figure 4.31 TLC fingerprinting and three-dimensional overlaid chromatogram of extracts, fractions and isolated compound from *Feronia limonia* stem bark at UV 366 nm.

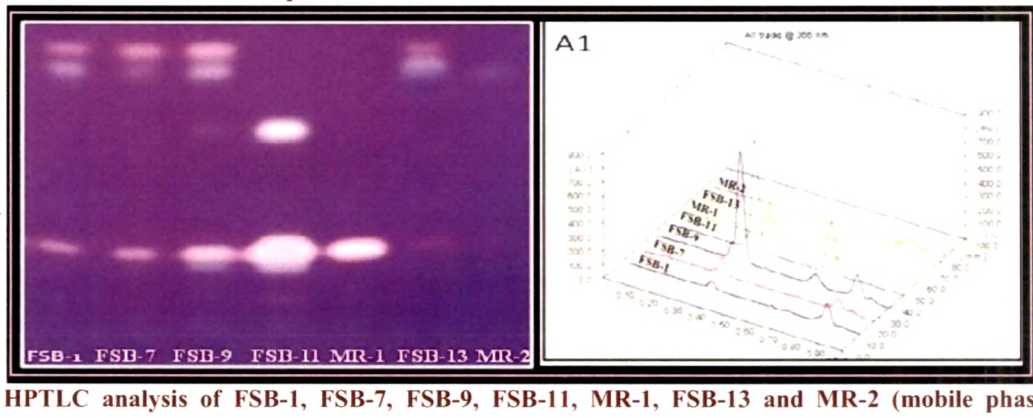

HPTLC analysis of FSB-1, FSB-7, FSB-9, FSB-11, MR-1, FSB-13 and MR-2 (mobile phase, hexane- chloroform- methanol; 1: 4.75: 0.25 Linomat V automatic applicator, detection; UV at 366 nm)

Figure 4.32 TLC fingerprinting and three-dimensional overlaid chromatogram of extracts, fractions and isolated compound from *Feronia limonia* stem bark at UV 366 nm.

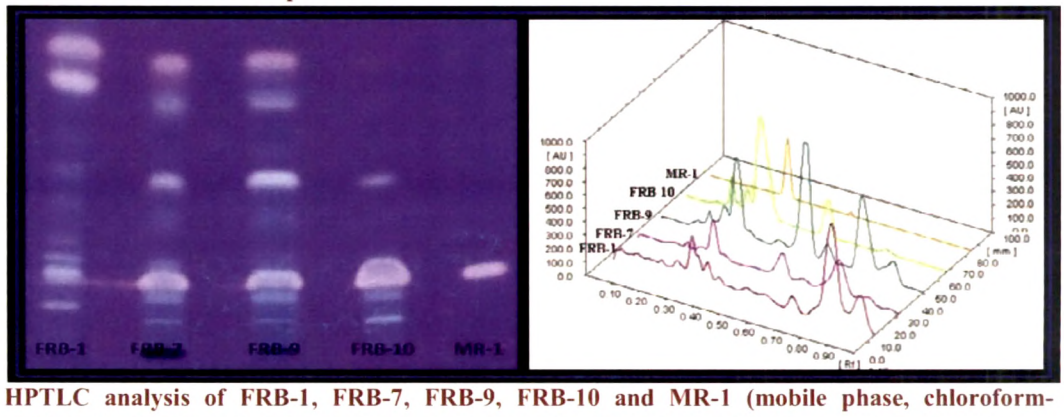

HPTLC analysis of FRB-1, FRB-7, FRB-9, FRB-10 and MR-1 (mobile phase, chloroform-methanol; 98: 2, Linomat V automatic applicator, detection; UV at 366 nm)

4.3.3 Analytical HPLC of isolated compound

4.3.3.a Analytical HPLC of MR-1

HPLC chromatography of isolated compound MR-1 was carried out using Hypersil reversed-phase C18 column. Analysis of MR-1 was isocratic at a 2 mL/min flow rate with methanol; water 45-55, v/v) as the mobile phase. Detection was carried out at 338 nm with retention time at 10.743 min with the flow rate 1 ml/min. The percentage purity of isolated compound was found to be 100%; HPLC chromatogram is shown in figure 4.33.

Figure 4.33 HPLC chromatogram of isolated compound MR-1

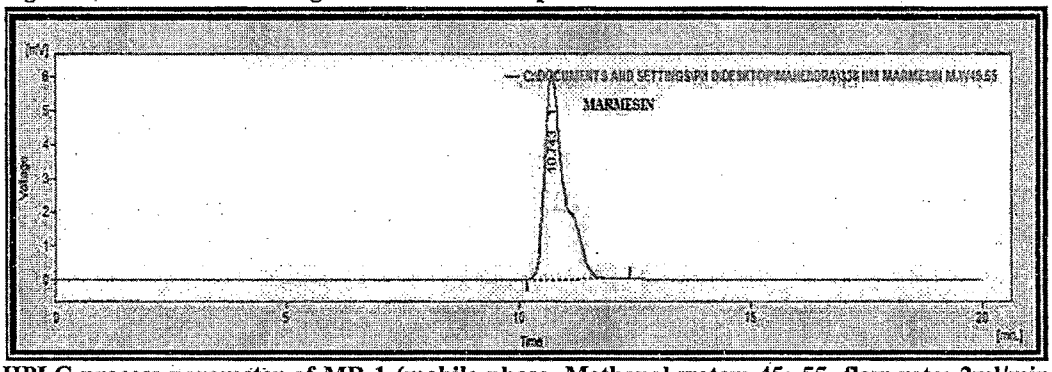

HPLC process parameter of MR-1 (mobile phase, Methanol-water; 45: 55, flow rate; 2ml/min, detection; UV at 338 nm, Retention time 10.743 minutes

4.3.3.b Analytical HPLC of MR-2

HPLC chromatography of isolated compound MR-2 was carried out using Hypersil reversed-phase C18 column, using mobile phase acetonitrile: 0.25% Acetic acid in water (50: 50). Detection was carries out at 265 nm with retention time at 6.360 min with the flow rate 2 ml/min. The percentage purity of isolated compound was found to be 96%; HPLC chromatogram is shown in figure 4.34.

Figure 4.34 HPLC chromatogram of isolated compound MR-2

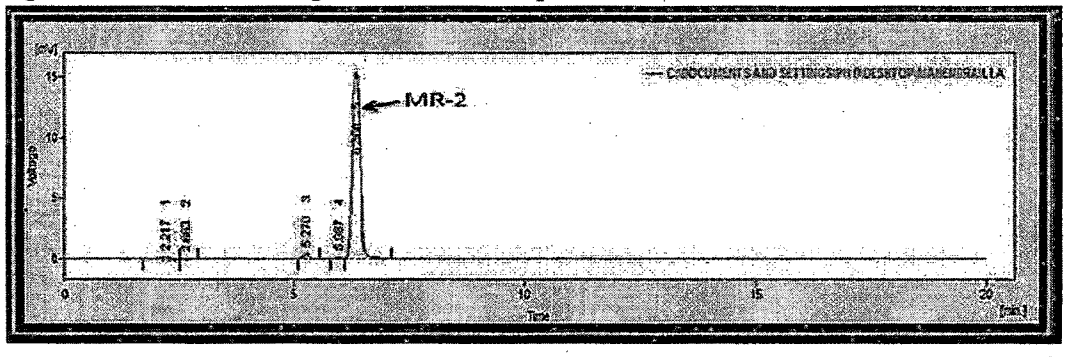

HPLC process parameter of MR-2 (mobile phase, Acetonitrile- 0.25% Acetic acid in water; 50: 50, flow rate; 2ml/min, detection; UV at 265 nm, Retention time 6.360 minutes

4.3.4 Phytochemical analysis of bioactive extracts, fraction from *F. limonia*

TLC assay provided qualitative insights into the bioactive constituents of the leaves stem bark and root bark of *Feronia limonia.* TLC characterization of total tannins (poly phenols) using n-butanol: acetic acid: water (40:1:5 v/v) and Ferric chloride reagent in FL-1, FL-7 and FL-9 shows 1, 10 and 5; FSB-7 shows 5; FRB-7 shows 6 yellowish black zones, respectively between the start and solvent front. Separation of flavanoids using ethyl acetate: formic acid: acetic acid: water (100:11:11:27) and Natural product reagent/PEG in FL-1, FL-7, FL-9 shows 1,9 and 3; FSB-7 shows 4 and FRB-7 shows 6 light and dark blue florescent spots, respectively. TLC pattern and chromatogram of leaves, stem bark and root bark are shown in Figures 4.35, 4.36 and 4.37, resp.

Figure 4.35 TLC fingerprinting and chromatogram for detection of total flavanoids in extracts and fractions of *Feronia limonia* leaves at UV 366 nm.

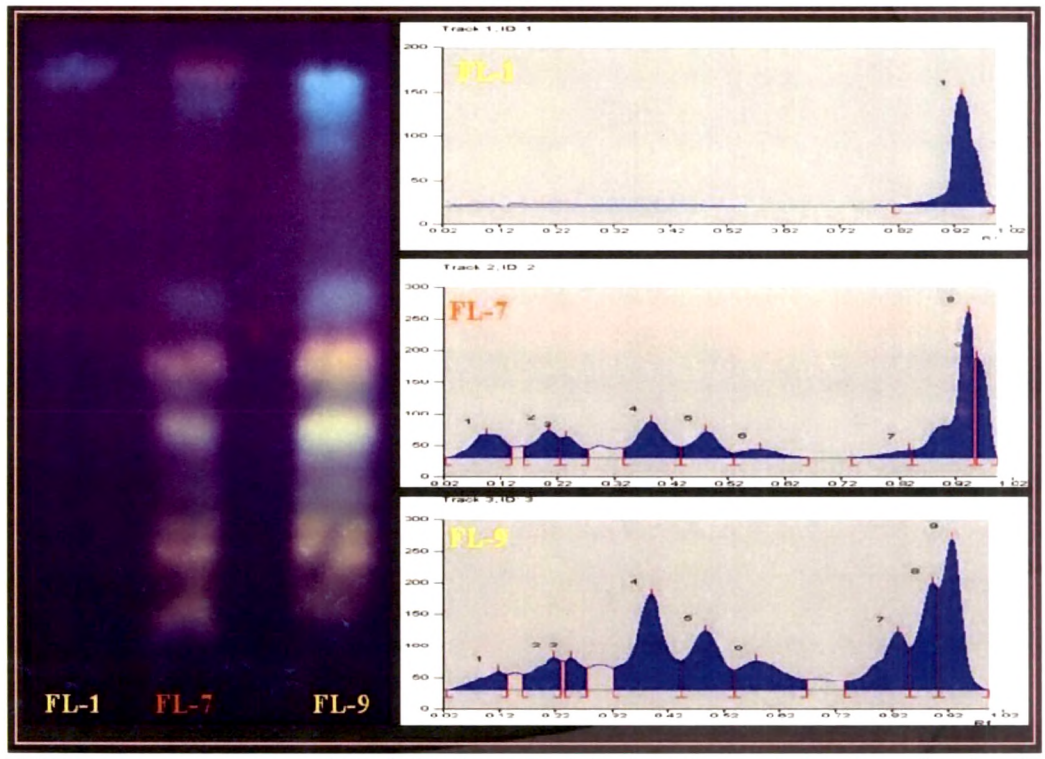

HPTLC process parameter of FL-1, FL-7 and FL-9 (mobile phase, ethyl acetate– formic acid–acetic acid–water 100:11:11:27; Natural product reagent/PEG, detection; UV at 366 nm

Figure 4.36 TLC fingerprinting and chromatogram for detection of total flavanoids in *Feronia limonia* stem bark extract at UV 366 nm.

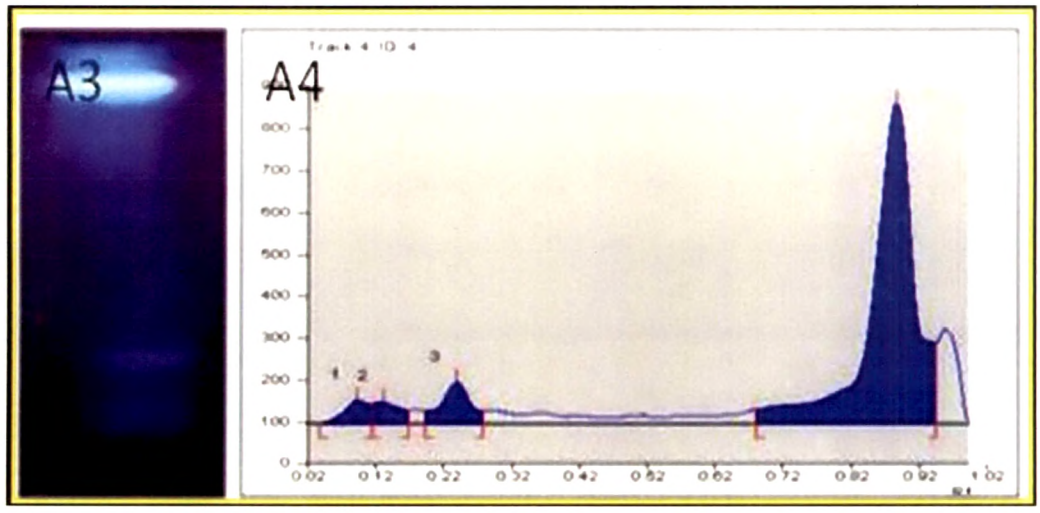

HPTLC process parameter of FSB-7 (mobile phase, ethyl acetate– formic acid–acetic acid–water 100:11:11:27; Natural product reagent/PEG, detection; UV at 366 nm)

Figure 4.37 TLC fingerprinting and chromatogram for detection of total flavanoids in *Feronia limonia* root bark extract at UV 366 nm.

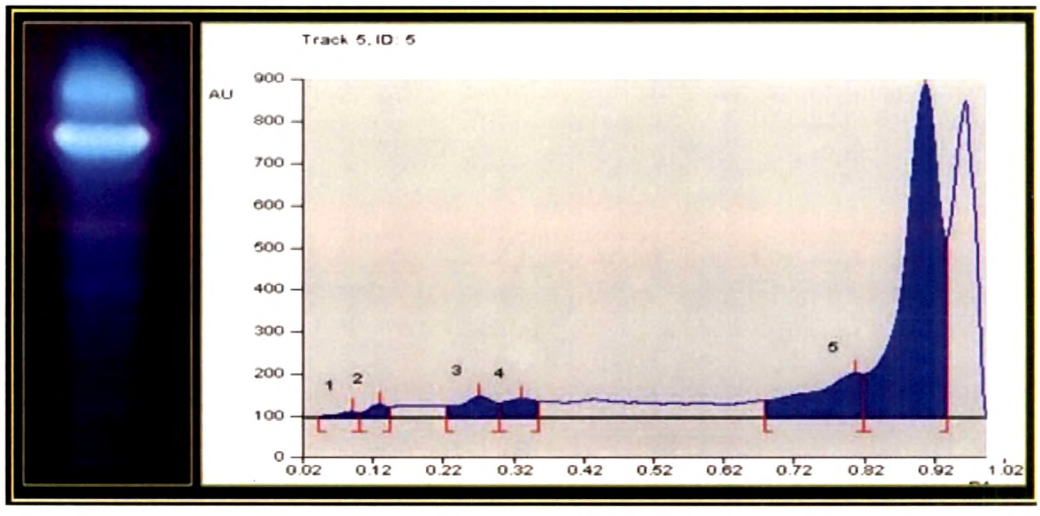

HPTLC process parameter of FRB-7 (mobile phase, ethyl acetate– formic acid–acetic acid–water 100:11:11:27; Natural product reagent/PEG, detection; UV at 366 nm)

4.3.5 Determination of content marker in methanolic extract of leaves, stem and root bark of *F. limonia* by HPTLC and HPLC

Marker compounds along with chromatographic profiles may be used to standardize the herbal raw materials. The clinical efficacy and pharmacological effects of a plant material will depend strongly on the amounts of biologically active ingredient present, and these must be accurately measured if a plant material is to be chemically standardized. Thus for the evaluation of identity and determination of quality of a

medicinal plant material a validated analytical method of analysis for the active ingredients has to be developed.

4.3.5.a Quantification of MR-1 from *Feronia limonia* stems bark by HPTLC

Reagents and Chemicals

All the chemicals, including solvents, were of analytical grade from E. Merck, India. The HPTLC plates Si 60F254 (20 cm · 20 cm) were purchased from E. Merck (Darmstadt, Germany).

Preparation of Crude Extract

Accurately weighed 5 g of the coarse powder of *Feronia limonia* stem bark were extracted separately with methanol (3 X 50 mL) under reflux (30 min each time) on a water bath. The combined extracts were filtered and concentrated, and transferred to a 25 mL volumetric flask and the volume was made up with methanol.

Preparation of Standard Solution

A stock solution of MR-1 (100 µg mL-1) was prepared by dissolving 1 mg of accurately weighed marmesin in methanol and making up the volume of the solution to 10 mL with methanol.

Chromatography

A Camag TLC system equipped with Camag Linomat V an automatic TLC sample spotter, Camag glass twin trough chamber (20 X 10 cm), Camag scanner 3 and integrated win CATS 4 Software were used for the analysis. TLC was performed on a pre-coated TLC plate silica gel 60F254 (20 cm X 20 cm). Samples and standards were applied on the plate as 8 mm wide bands with an automatic TLC sampler (Linomat V) under a flow of N_2 gas, 10 mm from the bottom and 10 mm from the side and the space between two spots were 15 mm of the plate. The linear ascending development was carried out in a Camag twin trough chamber (20 cm X 10 cm) which was presaturated with 20 mL mobile phase chloroform: methanol (9.5:0.5 v/v) for 20 min at room temperature (25 ± 2 ^{0}C and 40% relative humidity). The length of the chromatogram run was 8 cm. Subsequent to the development, TLC plates were dried under stream of hot air and then subjected to densitometric scanning using a Camag TLC scanner III (Camag, Switzerland) with win CATS software (version 1.4.1) in the absorbance- reflectance scan mode. Quantitative evaluation of the plate was performed in absorption-reflection mode at 338 nm. Quantification of MR-1 in the

extract of *F. Limonia* stem barks was performed by external standard method, using pure marmesin as standard.

Calibration Curve for MR-1

Stock solution of MR-1 (100 µg mL-1) was prepared in methanol and different amounts (20–100 ng spot^{-1}) were applied on a TLC plate, using Linomat V for preparing five point calibration graphs of peak area versus concentration. The regression equation for MR-1 was 1089.554 + 230.603x and co-relation coefficient (r) was 0.999.

Quantification of MR-1 in test Sample

Ten microlitres of sample solution were applied in triplicate on a TLC plate and developed, scanned as above. Peak areas were recorded and the amount of MR-1 was calculated using the calibration plot.

Specificity

The specificity of the method was ascertained by co-analyzing standard and sample. The band for marmesin in sample was confirmed by comparing the R_f (0.49) and absorption spectra of the spot to that of reference compound. The peak purity of MR-1 peak in sample track was assessed by comparing the spectra at peak start, peak apex and peak end positions of the band. Good correlation was also obtained between standards and sample overlay spectra ($r^2 > 0.99$).

Method Validation

The method was validated for precision, accuracy (ICH guideline., 1996-2005) and repeatability. Instrumental precision was checked by repeated scanning of the same spot 20 and 100 ng five times and was expressed as coefficient of variance (% RSD). Method precision was studied by analyzing the standards 20 and 100 ng per spot under the same analytical procedure and lab conditions on the same day and on different days (inter-day precision) and the results were expressed as % RSD. Accuracy of the method was tested by performing the recovery studies of the pre-analysed sample with standard at three levels (55.02, 68.78 and 82.53 µg mL^{-1}), % recovery and average % recovery were calculated.

System Suitability Test

Linearity and Detection Limit

Linearity was checked by applying standard solutions of MR-1 at five different concentration levels. The calibration curve was drawn in the concentration range of

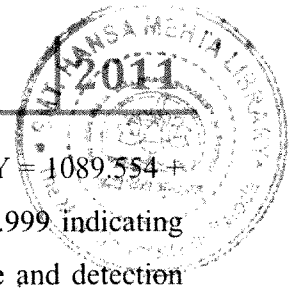

20–100 ng per spot. The equation for the calibration curve of MR-1 is Y = 1089.554 + 230.603x and the correlation coefficient of the calibration plot was 0.999 indicating good linearity. Results of regression analysis on the calibration curve and detection limits are presented in Table 4.9a.

Precision Studies

Instrumental precision was checked by repeated scanning of the same spots (20 and 100 ng per spot) of standard MR-1 five times and the RSD values were 1.56 and 1.82 for 20 and 100 ng per spot, respectively. To determine the precision of the developed assay method 20 and 100 ng per spot of the MR-1 standard was analysed five times within the same day to determine the intra-day variability. The RSD values were 3.41 and 6.29 for 20 and 100 ng per spot, respectively. Similarly the inter-day precision was tested on the same concentration levels on 2 days and the RSD values were 2.68 and 2.83, respectively (Table 4.9b).

Sample Analysis and Recovery Studies

This developed TLC method was subsequently applied for the analysis of MR-1 in the methanolic extract of *Feronia limonia* stem barks. The MR-1 content of the stem bark by this proposed method was found to be 0.03412%. For the examination of recovery rates, 80, 100 and 120% of pure MR-1 were added to preanalyzed sample and quantitative analysis was performed. The average recovery was 98.83 (Table 4.9c).

Table 4.9 Method validation parameter for quantification of MR-1 using proposed HPTLC Densitometric method.

(a) Linearity regression data

S. No.	Parameter	Results
1	RF	0.49
2	Dynamic range (ng per spot)	20–100
3	Equation	Y = 1089.554 + 230.603x
4	Slope	230.603
5	Intercept	1089.554
6	Limit of detection	5 ng
7	Limit of quantification	15.15 ng
8	Linearity (correlation coefficient)	0.999
9	Specificity	Specific

(b) Precision

Concentration (ng per spot)	Instrumental Precision (% RSD)	Method precision (% RSD)	
		Intra-day	Inter-day
20	1.56	3.41	2.68
100	1.82	6.29	2.83

(c) Recovery studies of MR-1

S. No.	Amount of MR-1 present in the sample (µg)	Amount of MR-1 added (µg)	Amount of MR-1 found (µg)	Recovery (%)
1	68.78	55.02	122.11	98.83
2	68.78	68.78	136.92	
3	68.78	82.53	148.81	

Figure 4.38 TLC chromatogram of methanolic extract of stem barks of *Feronia Limonia*

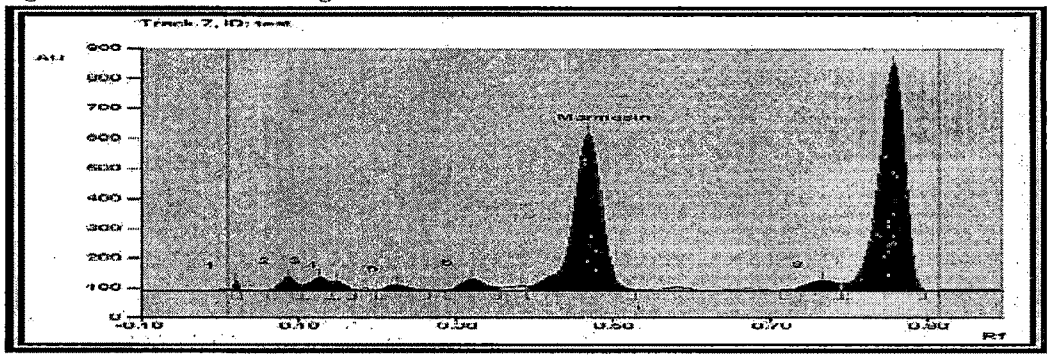

HPTLC process parameter of FSB-7 (mobile phase, chloroform– methanol 9.5: 0.5; detection; UV at 366 nm)

Figure 4.39 TLC chromatogram, for a standard MR-1 in methanol (Top left insert), Calibration curve and overlaid UV/VIS spectrum of standard track and sample track for MR-1

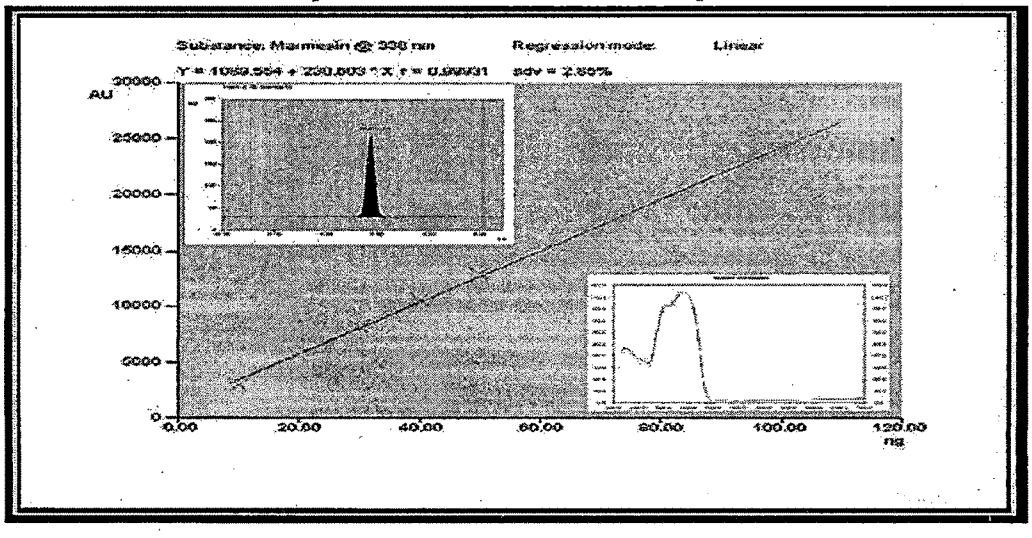

This developed TLC method was subsequently applied for the analysis of MR-1in the methanolic extract of *Feronia limonia* stem barks. The MR-1 content of the stem barks by this proposed method was found to be 0.03412 %w/w

4.3.5.b Identification and quantification of MR-1 from leaves, stem and root bark of *F. limonia* by HPLC

Instrumentation

The chromatographic system (Shimadzu, Kyoto, Japan) consisted of a Shimadzu LC-20 AT Prominence solvent delivery module, a manual Rheodyne injector (PerkinElmer, Mumbai, India) with a 20 mL fixed loop, and an SPD-20A Prominence (Shimadzu) UV-Vis detector. The separation was performed on a Hypersil C18 column (particle size 5 mm; 250 ′ 4.6 mm id; Thermoquest, Cheshire, UK) preceded by an ODS (Thermoquest) guard column (10 mm, 10 ′ 5 mm id) at an ambient temperature. Chromatographic data were recorded and processed using a Spinchrom Chromatographic Station® CFR Version 2.4.0.193 (Spinchrom Pvt. Ltd, Chennai, India). Peak purity analysis was carried out using an SPD M20A photo-diode array (PDA) detector from Shimadzu. Degassing of the mobile phase was done by sonication in an Ultrasonics Selec (DTC 503, Vetra, Italy) ultrasonic bath. An analytical balance from the AW series from Shimadzu was used with an accuracy of 0.01 mg.

Materials

Standard substance MR-1 was isolated in our laboratory (Jain et al, 2010) Acetonitrile, methanol, and water of HPLC grade were purchased from Qualigens (Mumbai, India). All the other solvents and reagents used were of analytical grade and were filtered through a 0.2 mm Ultipor® Nylon 66 membrane filter (Pall Life Sciences, East Hills, NY) prior to use.

Chromatographic Conditions

Chromatographic estimations were performed using an equilibrated Hypersil reversed-phase C18 column. Analysis of MR-1 was isocratic at a 2 ml/min flow rate with a methanol- water; 50: 50 v/v) as the mobile phase. The absorbance of MR-1 was good at 280 nm and it was free from any interference. The mobile phases were freshly prepared every day. The mobile phase was filtered through a 0.2 mm membrane filter to remove any particulate matter, mixed, and degassed by sonication before use. The

sensitivity of the detector was set at 0.01 absorbance units full scale (AUFS). Prior to injecting the solutions, the column was equilibrated for at least 60 min with the mobile phase flowing through the system.

Preparation of Standard Solutions

Approximately 5 mg standard MR-1 was weighed precisely in separate volumetric flasks and dissolved in 5 mL acetonitrile to obtain stock concentrations of 1000 µg/mL. Aliquots of each standard were further diluted to obtain solutions in the range of 20–100 µg /mL in methanol.

Method Validation

The methods developed for analyzing MR-1 individually were validated for linearity, accuracy, precision, specificity, and quantification limits as per ICH guidelines.

Figure 4.40 Calibration curve and HPLC chromatogram of isolated compound MR-1

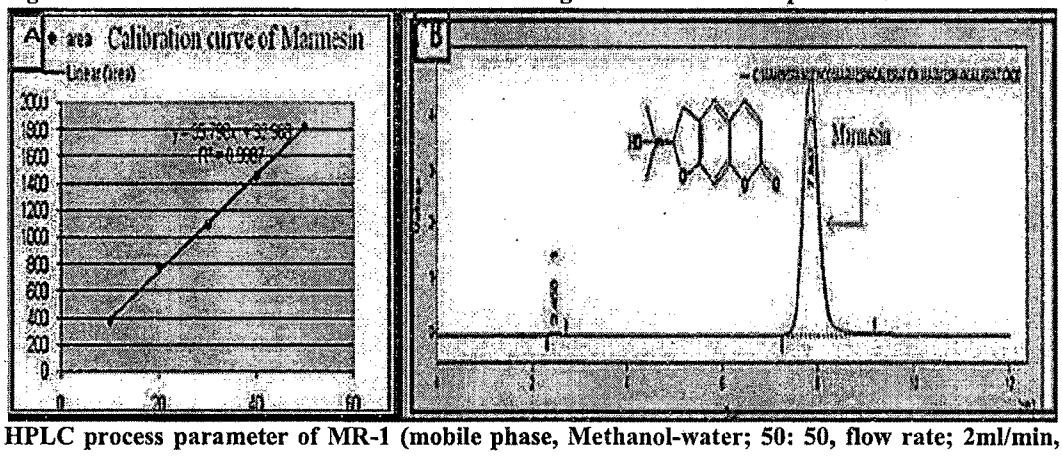

HPLC process parameter of MR-1 (mobile phase, Methanol-water; 50: 50, flow rate; 2ml/min, detection; UV at 280 nm, Retention time 7.743 minutes

Figure 4.41 HPLC chromatogram of FL-7 at UV 280 nm

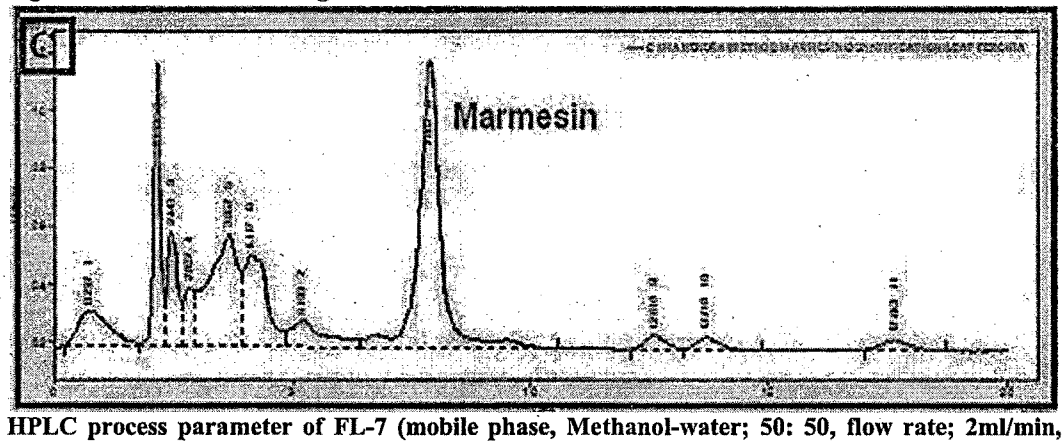

HPLC process parameter of FL-7 (mobile phase, Methanol-water; 50: 50, flow rate; 2ml/min, detection; UV at 280 nm, Total run time 20 minutes

Figure 4.42 HPLC chromatogram of FSB-7 at UV 280 nm

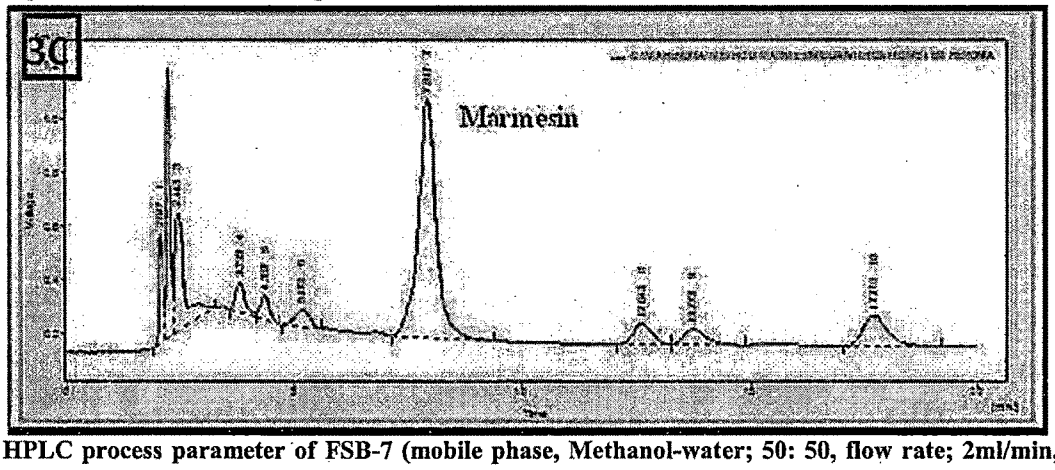

HPLC process parameter of FSB-7 (mobile phase, Methanol-water; 50: 50, flow rate; 2ml/min, detection; UV at 280 nm, Total run time 20 minutes

Figure 4.43 HPLC chromatogram of FRB-7 at UV 280 nm

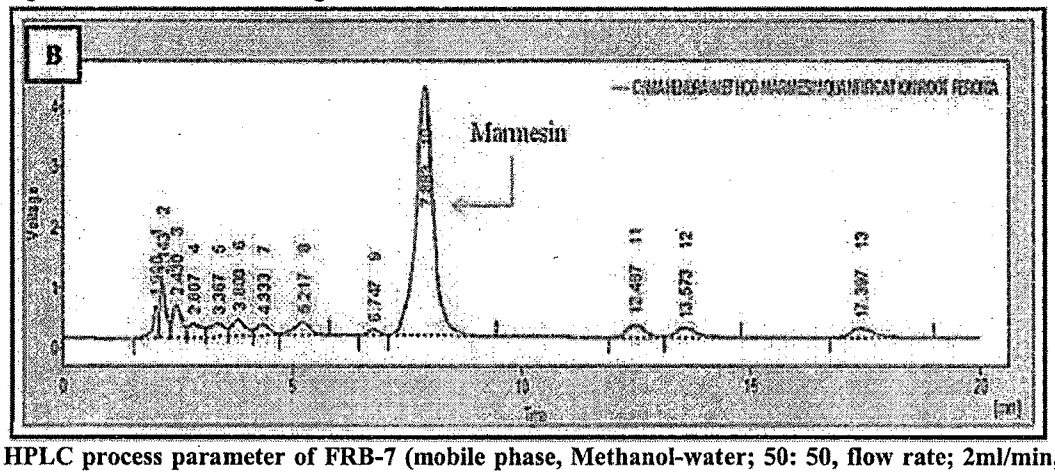

HPLC process parameter of FRB-7 (mobile phase, Methanol-water; 50: 50, flow rate; 2ml/min, detection; UV at 280 nm, Total run time 20 minutes

Calibration Curve (Linearity)

Linear regression analysis confirms that the r^2 values for both the drugs were 0.999, confirming the linear relationship between the concentration of the drugs and area under the curve (Table 1). The calibration curves (n = 3) constructed for the markers were linear over the concentration range of 20–100 μg/ml for each marker.

Precision and Stability

The precision results for the solution at the three concentrations are presented in Table 2. It was shown that the RSD values for retention time were <1%, while the RSD values for peak area were <2% for both intra- and interday assay precision (intraday, 4 h, six injections; interday, 6 days). For the stability test, the same sample was

analyzed within 24 h at room temperature, and the solution was found to be stable (RSD values for the retention time and peak area were both >3%).

Limit of Detection and Limit of Quantification

The LOD and LOQ were found to be 0.53 and 1.749 mg/ml, respectively, for PIN.

Specificity

Specificity evaluation was carried out by analyzing MR-1. It was observed that the peak of the drugs was well separated and was not interfered with by the degradation products and other components. Peak corresponding of the drugs showed positive values for the minimum peak purity index over the entire range of integrated chromatographic peaks, thus indicating the purity of the peaks (Table 3). Further, peak corresponding of the drug obtained by the proposed methods were seen to be pure (Figure 4.40). Thus, the methods were confirmed to be specific for the drug in the presence of the degradation products and other components.

Robustness

Table 4 shows the mean obtained (n = 6) for each factor studied, indicating that the selected factors remained unaffected by small variations of these parameters. The recovery obtained individually and the mean were between 98–101% for MR-1. Therefore, it can be concluded that the methods are consistent for detection wavelength, selected column, and solvent brand.

System Suitability

A system suitability test was performed to evaluate the chromatographic parameters [capacity factor, separation factor, column efficiency, number of theoretical plates, height equivalent to the theoretical plate (HETP) asymmetry of the peak, and resolution between two consecutive peaks] for each method before the validation runs (Table 5). Three replicate injections of the standard solution and three injections of the solution prepared for the specificity procedure were used.

Accuracy

As shown in Table 6, the recovery of the investigated component ranged from 98.17–99.69%, and their %RSD values were all <2%. It was known from recovery tests that the developed methods manifested reliability and accuracy for the measurement of the MR-1.

Table 4.10 Method validation parameter for quantification of MR-1 using proposed HPTLC Densitometric method.

a) Overview of method development for the quantitation of MR-1 in *Feronia limonia.*

Validation parameter	Results
HPLC Method	
Linearity range (μg mL^{-1})	20 – 100
Regression equation	Y=35.798x+32.968
Correlation coefficient	0.988
Limit of detection (LOD) (μg)	12.5
Limit of quantitation (LOQ) (μg)	20
System suitability	
Separation factor	1.60
Capacity factor	10.51
Tailing factor	1.41
Resolution factor	2.19

b) Intra- and inter-day precision of HPLC method

MR-1 (μg)	Intra-day		Inter-day	
	Mean (μg) (n=5)	RSD (%)	Mean (μg) (n=3)	RSD (%)
0.8	0.8034	1.01	0.7997	1.29
1.6	1.6014	0.56	1.6097	1.11
3.2	3.2010	0.40	3.2040	0.42

c) Recovery study (n=3)

Amount of MR-1 added (μg)	Amount of MR-1 recovered (μg)	Recovery (%)
50.00	49.08	98.2
75.00	74.10	98.9
100.00	100.17	100.2

d) Marmesin content (on plant dry weight basis) in *Ferinia limonia* by HPLC method (n=3)

Samples	HPLC Method
	MR-1 (mg/gm) (Mean ± SD)
Leaf	4.71 ± 0.02
Stem bark	4.91 ± 0.03
Root bark	20.86 ± 0.05

Applicability of the developed Method in leaves, stem bark and root bark of *Feronia limonia*

The developed methods were applied to the determination of MR-1 in the leaves, stem bark and root bark the results are presented in Table 4.10. The chromatogram obtained for FL-7 (Fig. 4.41), FSB-7 (Fig 4.42), FRB-7 (Fig 4.3) and MR-1 (Fig. 4.40) showed a separated instinct peak for marmesin. The calibration curve (Fig. 4.41) was prepared with marmesin and was found to be linear (R^2= 0.988) in the concentration range (10- 50µg/ml) used. The presence of MR-1 in FL-7, FSB-7 and FRB-7 were found to be 4.71 ± 0.02, 4.91 ± 0.03 and 20.86 ± 0.05 % w/w respectively.

4.3.6 Characterization of isolated compounds from *Feronia limonia*

4.3.6.a Characterization of MR-1

Compound MR-1 was identified as marmesin .Its structure is unambiguously elucidated by analysis of IR, ^{13}C NMR , Mass and CHNSO data (Figure 4.44). Its IUPAC name is [2,3-dihydro-2-(1-hydroxy-1 methylethyl)- 7H-furo[3, 2-g][1]benzopyran-7-one]. Molecular formula of marmesin is $C_{14}H_{14}O_4$ and its melting point is in between 188-190° C.

IR (KBR): ν_{max} 3479,2977, 2929, 1703, 1630, 1572, 14851444, 1404 and 819 cm-1 (Figure 4.45);1H NMR: δ1.23 and 1.37(> CMe2, 1.85(1H, br), 3.23 (2H, br d, *J* 8.8 Hz, H2-1'), 4.74 (1H, t, *J* 8.8 Hz, H-2'), 6.21(1H, d, *J* 9.5 Hz, H-3), 6.74(1H, s, H-8), 7.22(1H, s, H-5), 7.59(1H, d, *J* 9.5 Hz, H-4) (Figure 4.46) ; m/z (%) 246 (M+,39), 213(20), 188 (75), 187(100), 175(15), 160(30), 131(19), 59(66), 43(7) (Figure 4.47); CHO % elements- (Oxyzen-25.915), (Carbon-67.191) and (Hydrozen-5.480) (Figure 4.48).

Figure 4.44 Chemical structure of MR-1

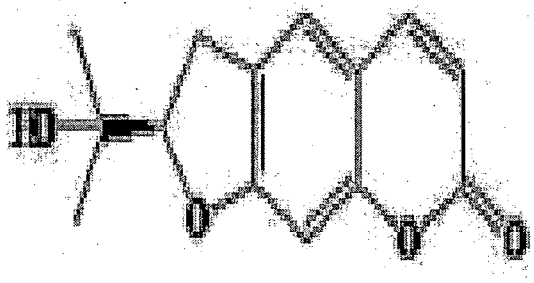

Marmesin

Marmesin is one of the most prevalent linear dihydrofuranocoumarin, is abundant in species belonging to the families of Umbelliferae, Apiaceae, Rutaceae, Moraceae, and Leguminoseae.[11,12]. It is originally isolated from indigenous indian plants, *Aegle marmelos Correa* [13], and later from the Hawiian shrub *Pelea barbigera* [14] both of these are from rutaceae family. It has an amazing array of scientifically acknowledged benefits for key areas of health, as dermal photosensitizing activity beneficial in the treatment of leucoderma [15], antifungal activity [16], phytoalexin [17], feeding deterrence effects [18] and radical scavenging activity [19].

Figure 4.45 IR spectrum of MR-1

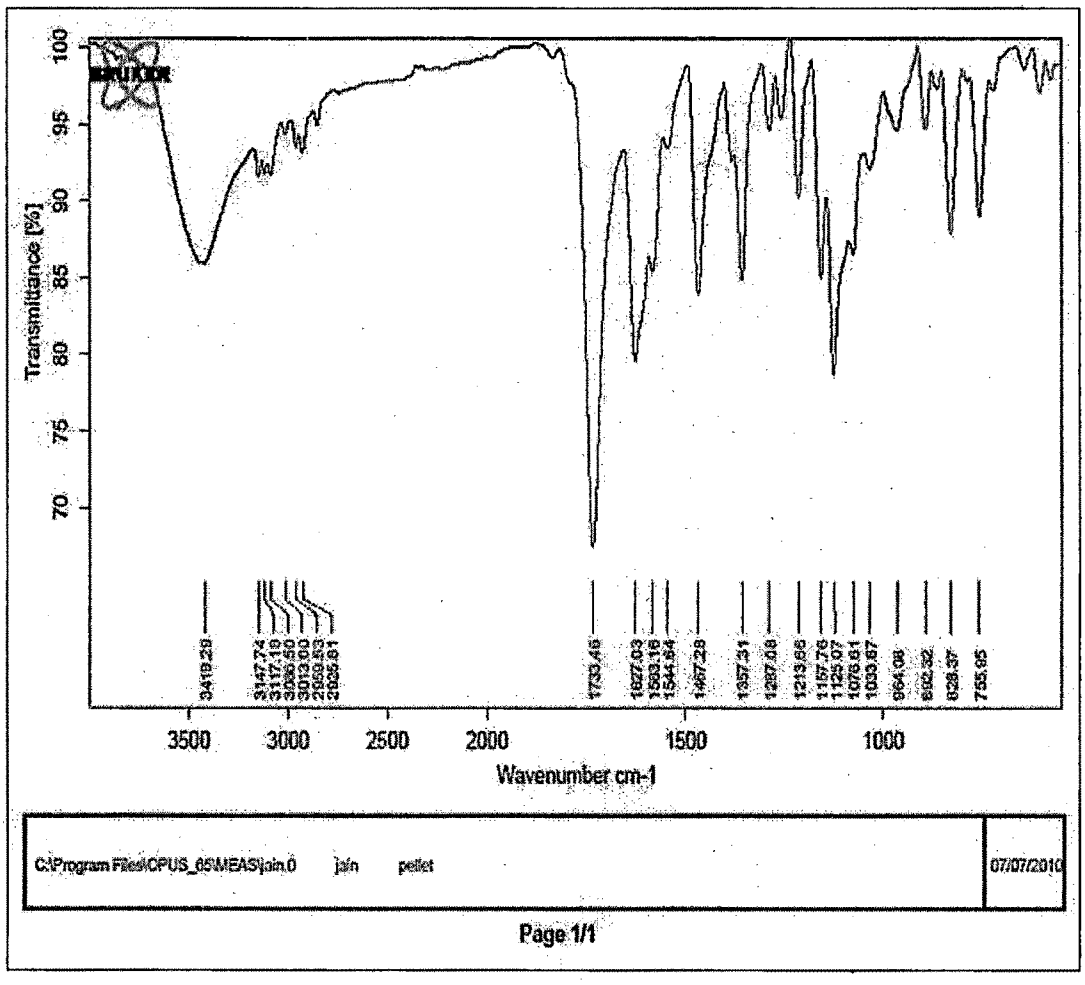

Figure 4.46 ^{13}C NMR of MR-1

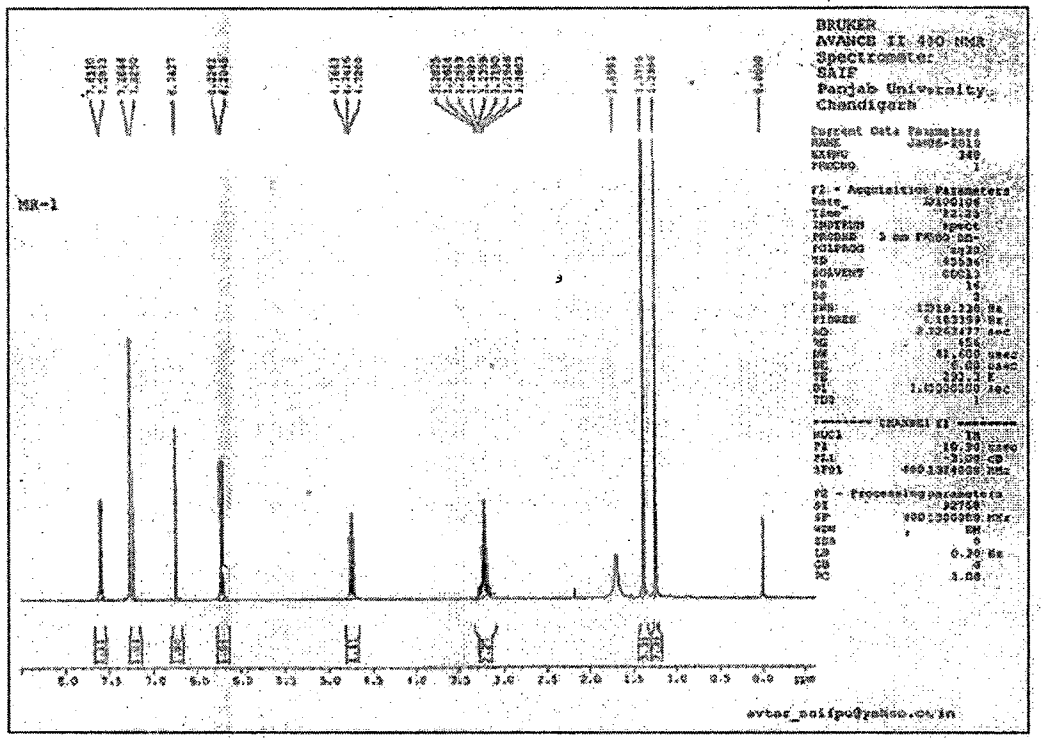

Figure 4.47 Mass spectrum of MR-1

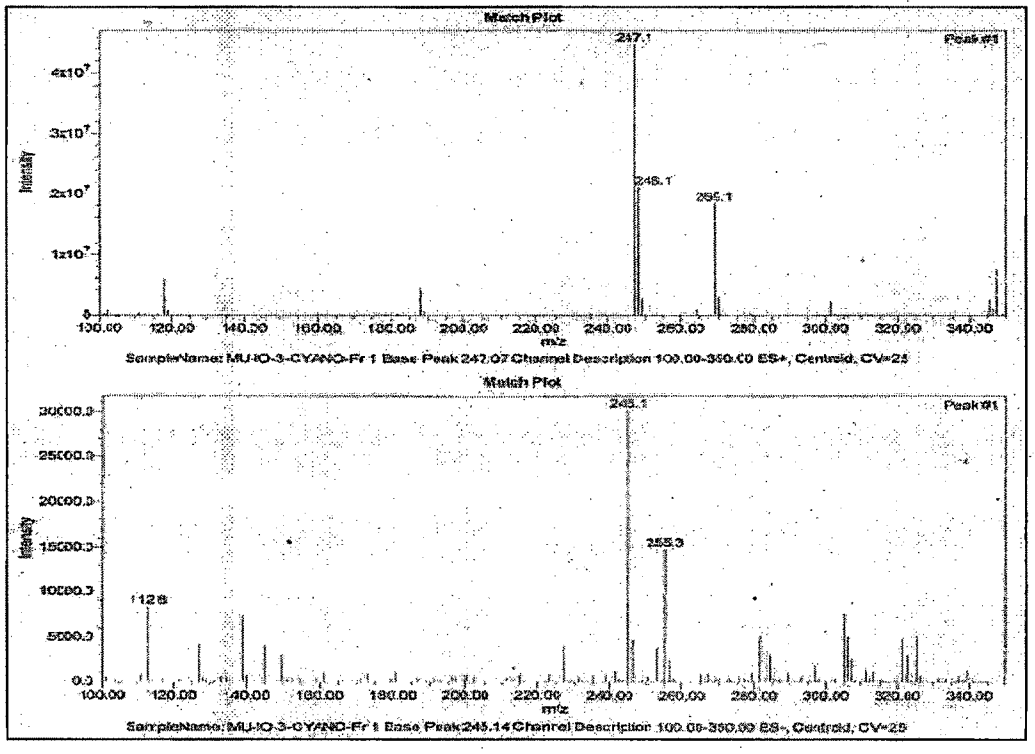

Figure 4.48 CHN analysis of MR-1

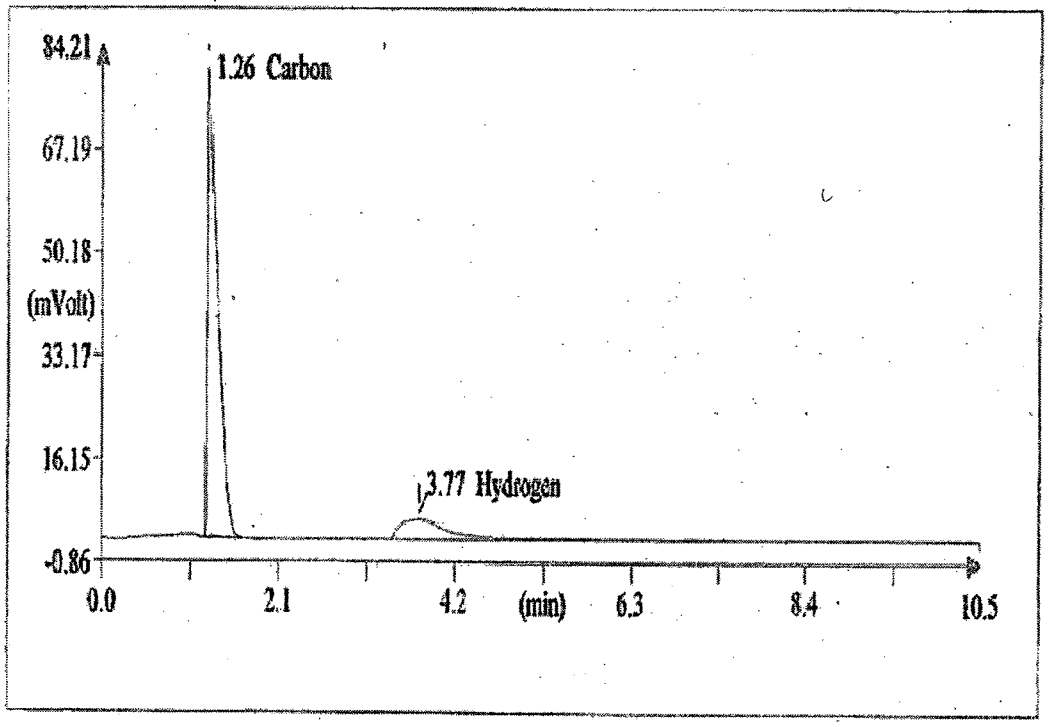

Figure 4.49 Oxygen analysis of MR-1

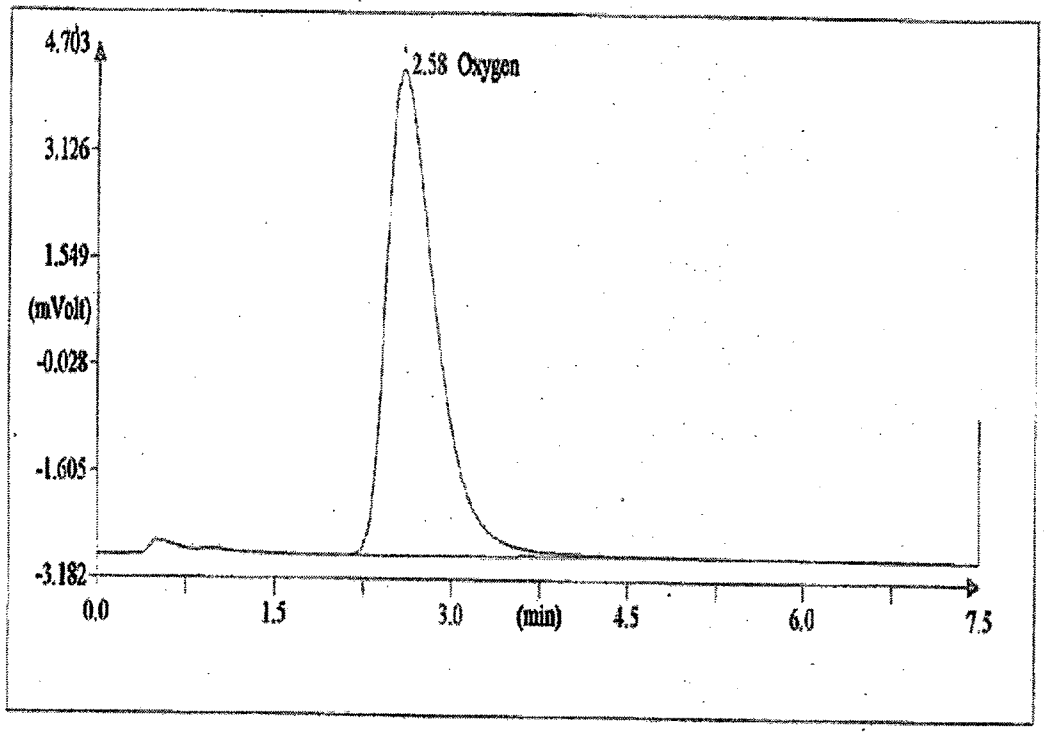

4.3.6.b Characterization of MR-2

Figure 4.50 Chemical structure of MR-2

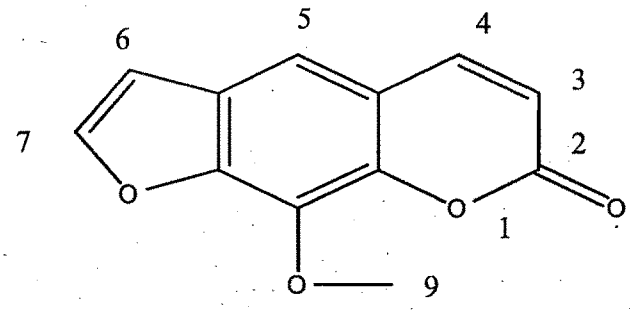

9-Methoxy-furo[3,2-g]chromen-7-one

Compound MR-2 was identified as 9-Methoxy- furo [3,2-g] chromen-7-one .Its structure is unambiguously elucidated by analysis of IR, ^{13}C NMR and Mass data (Figure 4.50). Its molecular weight is 216 and melting point is in between 176-179 ° C.

IR spectra of MR-2 is shown in Figure 4.51; Chemical shifts and multiplicity of MR-2 is given in Table 4.11 and Figure 4.52; Mass spectra is shown in Figure 4.47.

Figure 4.51 IR spectrum of MR-2

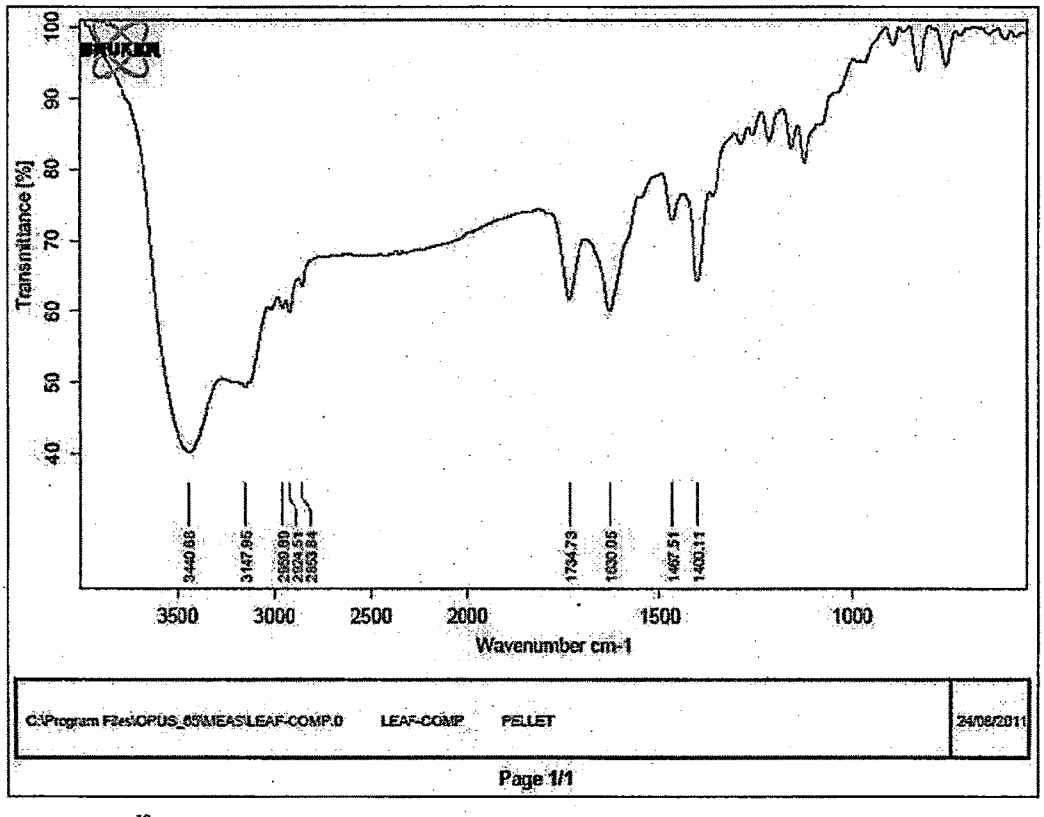

Figure 4.52 ^{13}C NMR of MR-2

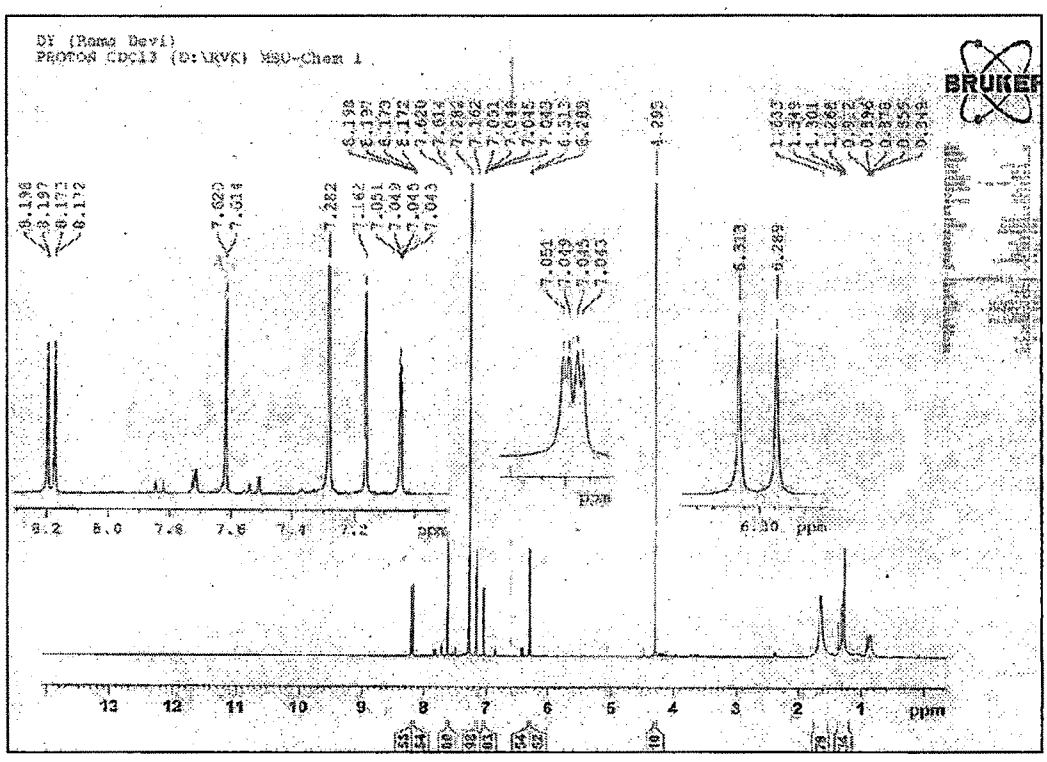

Table 4.11 Chemical shifts and multiplicity of MR-2 ^{13} C NMR spectra

Sr. No.	Multiplicity	Chemical shift
3-CH	Doublet	6.28-6.31
4-CH	Doublet	8.17-8.19
5-CH	Singlet	7.16
6-CH	Multiplet	7.04-7.05
7-CH	Doublet	7.61-7.62
9-CH_3	Singlet	4.29

Figure 4.53 Mass spectrum of MR-2

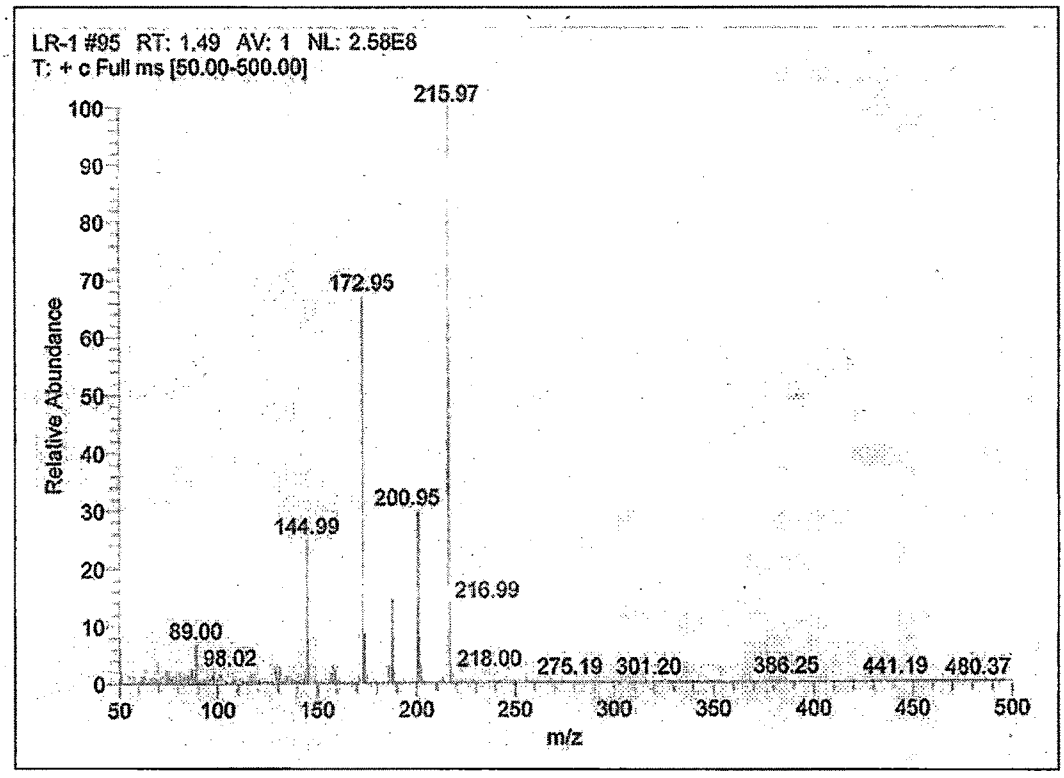

4.4 Biological studies

4.4.1 *In vitro* cytotoxicity studies of extracts, fractions and isolated compounds from *Feronia limonia*

In recent times *in vitro* cytotoxicity of plant extracts and bioassay guided fractions has gained importance for primary level screening. Prior to the therapeutic use of any herbal extract, it is imperative to perform a cytotoxicity assay. This is because crude extract of many herbs have been shown to be non-toxic but some of its bioassay guided fraction or pure compound may show toxicity (Tshikalange and Hussein, 2010). Human hepatoma cell line (Hep G2) is a popular and an effective *in vitro* model for assessing hepatoprotective potential of phytoconstituents or bioassay guided fractions due to its functional similarity with an intact liver.

4.4.1.a In vitro- cytotoxicity studies of Feronia limonia leaves (FLs)

In the present study, cytotoxicity evaluation was performed on leaves extracts, fractions and isolated compounds (FLs). Results of cytotoxicity assessment shows *Feronia limonia* petroleum ether extract (FL-1) and methanol extract (FL-7) revealed an identical pattern of cytotoxicity with both showing less that 50% cell

viability at 250 µg /ml dose. However methanolic fractions (FL-9, FL-10 or FL-11) showed a differential pattern of cytotoxicity of Hep G2 cells. FL-9 exhibited superior percentage of cell viability (65%) at 200µg/ml. However FL-10 and FL-11 recorded significant cytotoxicity, which was characterized by less than 50% cell viability at all the doses studied herein. MR-2 recorded much improved cell viability as compared to its preceding fractions (Figure 4.54).

4.4.1.b Cytotoxicity assessment of Feronia limonia stem bark (FSBs)

Cytotoxicity evaluation on stem bark extracts, fractions and isolated compounds (FSBs), was performed in the dose range of 10- 1000µg/ml. Cytotoxicity assessment of FSB-1, FSB-7, FSB-11, MR-1 and MR-2 revealed an identical pattern of cytotoxicity that was marked by greater than 50% viable cells at 250 µg /ml dose. However FSB-9 and FSB-13 showed relatively high toxic pattern as compared to other samples studied herein. The MTT assay of pure compounds (MR-1and MR-2) revealed that they were non toxic up to 250 µg/ml dose. These results were the basis on which a detailed investigation was initiated in *in vitro* and *in vivo* experimental models (Figure 4.55).

4.4.1.c In vitro cytotoxicity assessment of Feronia limonia root bark (FRBs)

As herbal extracts and compounds are often known to contain natural toxicant extracts, fractions and compounds from root barks (FRBs) were evaluated for their possible cytotoxicity. The observation clearly suggested that FRB-7 and MR-1 showed maximum cell viability as compared to the (FRB-1, FRB-9 and FRB-10) other experimental samples. However, FRB-7 shows good cell viability pattern at 250 µg/ml dose. They were non toxic up to 200 µg/ml dose, so these results provide an impetus for detailed investigation of their hepatoprotective potentials. Cytotoxicity assessment of FRBs extract, fractions and MR-1 are shown in Figure 4.56.

Figure 4.54 Cytotoxicity evaluation of extracts, fractions and isolated compound from *Feronia limonia* leaves

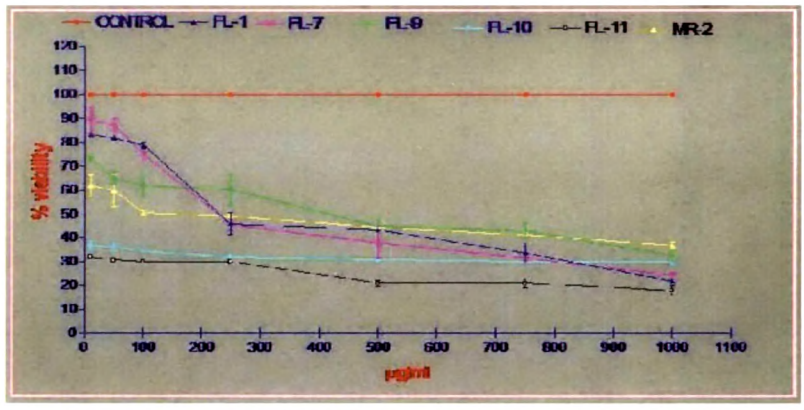

Graphical representation of MTT assay for FL-1, FL-7, FL-9, FL-10, FL-11 and MR-2 at concentration10-1000µg/ml

Figure 4.55 Cytotoxicity evaluation of extracts, fractions and isolated compound from *Feronia limonia* stem bark

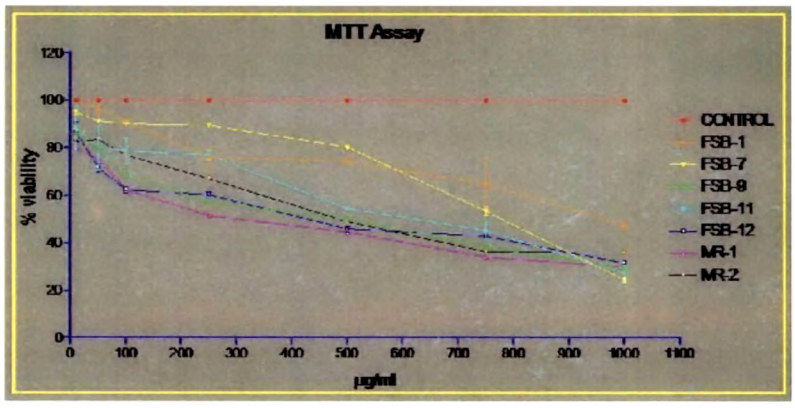

Graphical representation of MTT assay for FSB-1, FSB-7, FSB-9, FSB-11, FSB-12, MR-1 and MR-2 at concentration10-1000µg/ml

Figure 4.56 Cytotoxicity assessment of extracts, fractions and isolated compound from *Feronia limonia* root bark

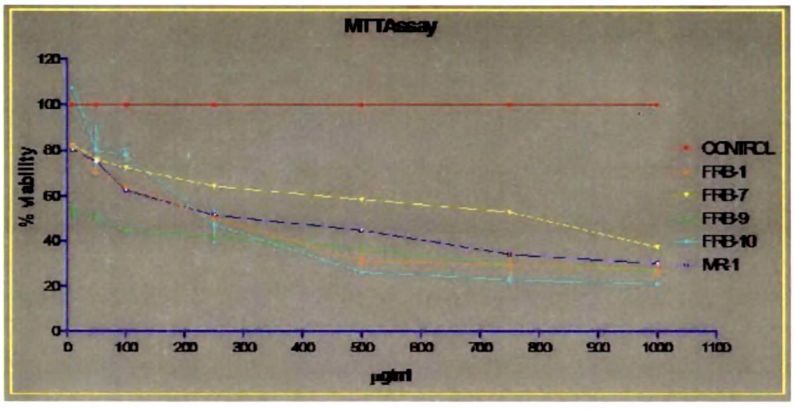

Graphical representation of MTT assay for FRB-1, FRB-7, FRB-9, FRB-10 and MR-1 at concentration10-1000µg/ml

4.4.2 In vitro Hepatoprotective potential of leaves, stem bark and root bark of *Feronia limonia*

Carbon tetrachloride (CCl_4) is a well-known hepatotoxicant that causes necrotic damage to cells and tissue, resulting in leakage of transaminases enzymes (SGOT and SGPT) into the blood stream. High concentrations of CCl_4 *in vivo* can manifest extensive toxic damages to hepatocytes via generation of trichloromethyl free radicals (CCl_3* and/or CCl_3OO*) that induce biotransformation by hepatic microsomal Cytochrome P 450 (Jadeja et al., 2011; Ree and Spector, 1961)). HepG2 cell line is a popular *in vitro* model where in, cells are subjected to CCl_4 induced toxicity and subsequent amelioration using a desired herbal extract or compound is question (Sathaye et al., 2010). Therefore herein FLs, FSBs and FRBs (which are found to be non-toxic after previous cytotoxicity studies) are evaluated for their hepatoprotective potential by using HepG2 cell lines.

4.4.2 a In vitro hepatoprotective potential of Feronia limonia leaves

Activity levels of SGOT and SGPT in cell supernatants revealed that there was a significant increment in their activity levels in cells treated with 1% CCl_4. On evaluating FLs for hepatoprotection results indicate that FL-7 (methanolic extract) provides superior hepatoprotection as compared to FL-1. This could be because of the presence of higher amounts of coumarins and flavanoids in methanolic extract which is also found out by El-Khrisy et al., 1994. Positive results obtained with FL-9 are also contributable to the same reason. However, cytotoxicity obtained in FL-10 and FL- 11 is inexplicable and warrants further study. Furthur, FL-9 (fraction) imparted superior hepatoprotection than FL-7 which could possibly be because of the flavanoids and coumarins higher concentration, due to fractionation. MR-2 is found to be non- toxic and hepatoprotective,which could be attributed to the possible removal of the unknown toxic substance in the insoluble fraction (Table 4.12).

As, a whole, co-supplementation of FL-1, FL-7, FL-9 or MR-2 recorded a non-linear dose dependent decrease in levels of SGOT and SGPT. Reduction in the levels of SGOT and SGPT towards the respective normal value is an indication of repair of hepatic tissue damages caused by CCl_4 (Ree and Spector, 1961).

These activity levels were comparable to that of dose dependent decrease observed in CCl_4 and sylimarin treated groups.

Table 4.12 Effect of *F.limonia* leaf extracts, fractions, isolated compound (MR-2) and sylimarin on CCL_4 induced hepatotoxicity

TREATMENTS		SGOT (IU/l)	SGPT (IU/l)	CELL VIABILITY(%)
Control		5.00±0.57	4.00±0.88	100
1% CCL_4		10.00±3.46###	8.55.00±1.78###	20.81±1.21###
1% CCL_4 + Sylimarin (µg/ml)	10	6.33±0.33**	5.33±0.88**	74.28±1.70***
	20	6.33±0.66**	3.33±0.66***	81.17±1.99***
	50	4.00±0.57***	2.66±0.88***	84.41±1.87***
	100	4.00±1.00***	2.66±0.33***	94.54±4.10***
	200	3.33±0.88***	2.33±0.88***	96.85±3.45***
1% CCL_4 + FL-1 (µg/ml)	10	7.33±0.88*	6.66±1.00**	84.06±2.00***
	20	7.00±0.57**	3.00±0.57***	84.43±4.99***
	50	5.00±0.58***	2.33±0.66***	78.48±5.49***
	100	3.66±0.88***	2.12±0.57***	76.79±6.29***
	200	2.33±0.88***	2.03±0.33***	79.60±8.00***
1% CCL_4 + FL-7 (µg/ml)	10	7.00±0.57*	4.66±1.1***	87.85±4.32***
	20	6.33±0.88**	4.33±0.89***	85.18±1.93***
	50	3.33±0.88***	3.33±0.66***	85.56±2.29***
	100	3.00±0.58***	3.00±0.57***	78.01±4.12***
	200	2.66±0.33***	2.66±0.33***	77.40±3.46***
1% CCL_4 + FL-9 (µg/ml)	10	7.66±0.67*	4.66±0.66***	90.13±2.08***
	20	5.00±0.58**	3.20±0.57***	98.82±2.78***
	50	4.00±0.56***	3.13±0.42***	85.23±3.23***
	100	3.00±0.44***	2.33±0.33***	87.57±1.44***
	200	2.33±0.34***	2.03±0.33***	88.65±2.81***
1% CCL_4 + MR-2 (µg/ml)	10	7.00±0.65*	7.6±0.88*	54.21±2.00**
	20	6.00±1.00**	6.00±0.57**	65.13±1.16***
	50	6.33±0.88**	6.66±0.88**	83.02±2.11***
	100	4.12±0.65***	4.22±0.32***	83.40±2.79***
	200	3.11±0.23***	2.00±0.21***	85.48±2.99***

Data expressed as mean± S.E.M. for n=3. Where, ###p<0.001 compared to control and *p<0.05, **p<0,01 and ***p<0.001 compared to 1%CCL_4.

4.4.2.b In vitro hepatoprotective potential of Feronia limonia stem bark

When, FSBs (FSB-1, FSB-7, FSB-9, FSB-11and FSB-13) and MRs (MR-1 and MR-2) were subjected to scrutiny for assessing their hepatoprotective potentials results revealed that FSB-7, FSB-9, MR-1 and MR-2 imparted hepatoprotection. There is significant increment in the levels of SGOT and SGPT in cell supernatants of cells

treated with 1% CCl_4. However, co-supplementation of FSB-1, FSB-7.FSB-9, MR-1 and MR-2 recorded a non-linear dose dependent decrease in activity levels of SGOT and SGPT that were comparable to dose dependent decrease observed in CCl_4 + sylimarin treated groups (Table 4.13).

Table 4.13 Effect of *Feronia limonia* extracts, fractions, isolated compound (MR-1 and MR-2) and sylimarin on CCL_4 induced hepatotoxicity

TREATMENTS		SGOT (IU/l)	SGPT (IU/l)	CELL VIABILITY (%)
Control		5.00±0.57	4.00±0.88	100
1% CCL_4		11.00±3.46$^{###}$	9.22±1.78$^{###}$	20.81±1.21$^{###}$
1% CCL_4 + Sylimarin (µg/ml)	10	6.33±0.33**	5.33±0.88**	74.28±1.70***
	20	6.33±0.66**	3.33±0.66***	81.17±1.99***
	50	4.00±0.57***	2.66±0.88***	84.41±1.87***
	100	4.00±1.00***	2.66±0.33***	94.54±4.10***
	200	3.33±0.88***	2.33±0.88***	96.85±3.45***
1% CCL_4 + FSB-1 (µg/ml)	10	6.33±0.66***	6.66±0.88***	90.71±2.53***
	20	5.33±0.33***	5.66±0.33***	95.40±0.61***
	50	4.66±0.33***	4.33±0.33***	99.34±0.72***
	100	3.66±0.66***	3.66±0.88***	86.02±1.34***
	200	3.00±0.57***	2.33±0.33***	86.26±1.25***
1% CCL_4 + FSB-7 (µg/ml)	10	8.00±0.57*	5.00±1.15***	95.82±2.86***
	20	5.33±0.33***	6.00±0.57***	96.39±1.00***
	50	4.33±0.33***	5.66±0.33***	88.18±1.73***
	100	2.66±0.88***	2.66±0.66***	91.74±4.03***
	200	2.33±0.33***	2.33±0.33***	86.96±2.23***
1% CCL_4 + FSB-9 (µg/ml)	10	10.66±1.33^{NS}	7.00±0.57*	97.74±0.24***
	20	8.33±0.88*	6.33±0.88**	83.02±4.15***
	50	5.00±0.57***	4.66±0.88***	86.16±4.36***
	100	3.66±0.33***	3.00±1.15***	81.76±4.97***
	200	3.66±0.33***	2.33±0.88***	90.62±0.16***
1% CCL_4 + FSB-11 (µg/ml)	10	9.66±1.45^{NS}	7.66±0.33^{NS}	86.35±1.48***
	20	8.33±0.33*	8.33±0.33^{NS}	76.41±3.44***
	50	10.33±0.88^{NS}	6.60±0.33^{NS}	71.26±2.27***
	100	7.33±0.33*	7.33±1.20^{NS}	67.65±1.48**
	200	7.66±0.88*	7.00±0.57^{NS}	52.49±1.86**
1% CCL_4 + FSB-12 (µg/ml)	10	10.33±0.33^{NS}	8.33±0.33^{NS}	34.40±0.70*
	20	9.00+0.57^{NS}	6.00±0.57**	41.52±0.99*
	50	8.33±0.88*	6.00±1.15**	67.96±0.89**
	100	2.66±0.33***	3.33±0.88***	75.64±0.39***
	200	4.00±0.57***	4.66±0.33***	52.88±0.29**
1% CCL_4 +	10	7.33±0.33**	7.66±0.88*	44.21±2.03*
	20	5.33±0.88***	6.00±0.57***	55.13±0.16**

MR-1 (µg/ml)	50	6.66±0.33***	5.00±0.57***	83.02±5.79***
	100	4.00±0.57***	3.00±0.57***	83.40±2.99***
	200	3.00±0.57***	2.00±0.57***	85.84±2.96***
1% CCL_4 + MR-2 (µg/ml)	10	7.00±0.65*	7.6±0.88*	54.21±2.00**
	20	6.00±1.00**	6.00±0.57**	65.13±1.16***
	50	6.33±0.88**	6.66±0.88**	83.02±2.11***
	100	4.12±0.65***	4.22±0.32***	83.40±2.79***
	200	3.11±0.23***	2.00±0.21***	85.48±2.99***

Data expressed as mean± S.E.M. for n=3. Where, $^{###}p<0.001$ compared to control and *p<0.05, **p<0,01 and ***p<0.001 compared to 1%CCL_4.

4.4.2.c In vitro- Hepatoprotective potential of Feronia limonia root bark

FRBs and MR-1 were investigated for their possible *in vitro* hepatoprotective potential in the dose range of 10-200 µg/ml doses. Activity levels of AST, ALT in cells supernatant treated with FRBs and MR-1 revealed that FRB-1, FRB-9 and FRB-10 provided hepatoprotection up to 50 µg/ml and failed to do so at higher dose. In contrast, FRB-7 and MR-1 reported significant decrement in activity level of SGOT and SGPT level even at higher doses. Thus, co-supplementation of FRB-7 and MR-1 is more potent in preventing CCl_4 induced leakage of SGOT, SGPT and improved cell viability compared to FRB-1, FRB-9 and FRB-10 (Table 4.14).

Table 4.14 Effect of FRBs and sylimarin on CCL_4 induced hepatotoxicity

TREATMENTS		SGOT (IU/l)	SGPT (IU/l)	CELL VIABILITY (%)
Control		5.00±0.57	4.00±0.88	100
1% CCL_4		11.00±3.46$^{###}$	10.00±1.78$^{###}$	20.81±1.21$^{###}$
1% CCL_4 + Sylimarin (µg/ml)	10	6.33±0.33**	5.33±0.88**	74.28±1.70***
	20	6.33±0.66**	3.33±0.66***	81.17±1.99***
	50	4.00±0.57***	2.66±0.88***	84.41±1.87***
	100	4.00±1.00***	2.66±0.33***	94.54±4.10***
	200	3.33±0.88***	2.33±0.88***	96.85±3.45***
1% CCL_4 + FRB-1 (µg/ml)	10	6.66±0.88***	5.33±1.52**	44.46±0.49*
	20	3.66±0.66***	5.33±0.33**	77.00±0.29***
	50	3.00±0.57***	6.33±.20***	99.34±0.72***
	100	11.00±0.57^{NS}	5.66±1.20**	86.02±1.34***
	200	9.00±0.57^{NS}	8.00±0.57^{NS}	86.26±1.25***
1% CCL_4 +	10	4.33±0.88***	3.66±0.88***	95.82±2.86***
	20	3.66±0.88***	2.00±0.66***	96.39±1.00***

FRB-7 (µg/ml)	50	2.66±0.33***	3.33±0.57***	88.18±1.73***
	100	2.66±0.33***	2.33±0.33***	91.74±4.03***
	200	2.66±0.66***	2.00±0.57***	86.96±2.23***
1% CCL_4 + FRB-9 (µg/ml)	10	3.33±0.66***	9.00±0.57 ^{NS}	97.74±0.24***
	20	6.66±0.88**	9.00±0.57 ^{NS}	83.02±4.15***
	50	6.33±0.88**	7.66±0.66*	86.16±4.36***
	100	10.33±0.88 ^{NS}	7.00±0.57*	81.76±4.97***
	200	10.00±0.57 ^{NS}	6.66±0.88**	90.62±0.16***
1% CCL_4 + FRB-10 (µg/ml)	10	4.00±0.57***	10.00±0.57 ^{NS}	86.35±1.48***
	20	5.00±0.57***	9.00±0.57 ^{NS}	76.41±3.44***
	50	7.00±1.00**	7.33±1.20 ^{NS}	71.26±2.27***
	100	8.66±1.20 ^{NS}	7.00±0.57*	67.65±1.48***
	200	10±0.57 ^{NS}	8.00±0.57 ^{NS}	52.49±1.86**
1% CCL_4 + MR-1 (µg/ml)	10	7.33±0.33 ^{NS}	7.66±0.88*	44.21±2.03*
	20	5.33±0.88***	6.00±0.57***	55.13±0.16**
	50	6.66±0.33**	5.00±0.57***	83.02±5.79***
	100	4.00±0.57***	3.00±0.57***	83.40±2.99***
	200	3.00±0.57***	2.00±0.57***	85.84±2.96***

Data expressed as mean± S.E.M. for n=3. Where, $^{###}$p<0.001 compared to control and *p<0.05, **p<0,01 and ***p<0.001 compared to 1%CCL_4.

4.4.3 Acridine orange/ethidium bromide (fluroscent dye) staining of *Feronia limonia*

Two DNA intercalators, acridine orange (AO) and ethidium bromide (EB) were used to visualise condensed chromatin of apoptotic dead cells. The differential uptake of these two dyes allows the identification of live and dead cells. While the cationic dye acridine orange enters into live cells containing normal nuclear chromatin and exhibit green colour, ethidium bromide is excluded by live cells and it stains fragmented nuclear chromatin in apoptotic cells in orange colour. These staining studies and photographic morphological evidence will further help in evaluating the hepatoprotective potential of various extracts, fractions and compounds of *Feronia limonia.*

4.4.3.a AO/EB staining and cell morphology study on FLs

A detailed scrutiny of AO and EB positive cells in the control and treated groups revealed that CCl_4 treatment accounted for maximum number of EB positive cells whereas the control group recorded AO positive cells. Also more number of AO

positive cells were recorded in CCl_4 + FL-1, FL-7, FL-9 groups followed by CCl_4+ MR-2 group as compared to CCl_4 treated groups, CCl_4 +SYL group recorded maximum AO positive cells with result of this group comparable to that of control group. Similar set of results were observed in morphological changes of HepG2 cells (Figure 4.57).

4.4.3.b AO/EB staining and cell morphology study on FSBs

In FSBs also, CCl_4 treatment accounted for maximum number of EB positive cells whereas the control group recorded for more AO positive cells. In case of, CCl_4+FSB-7 group, more number of AO positive cells than CCl_4 treated group were recorded. But, CCl_4 +SYL group recorded maximum AO positive cells. Similar set of results were observed in morphological changes of HepG2 cells (Figure 4.58).

4.4.3.c AO/EB staining and cell morphology study on FRBs

In FSBs also, CCl_4 treatment accounted for maximum number of EB positive cells whereas the control group recorded for more AO positive cells. More number of AO positive cells were recorded in CCl_4 + FRB-7 group followed by CCl_4 + MR-1 group as compared to CCl_4 treated groups, CCl_4 +SYL group recorded maximum AO positive cells with result of this group comparable to that of control group. Similar set of results were observed in morphological changes of HepG2 cells (Figure 4.59).

Figure 4.57 Phase contrast and AO/ EB stained photomicrographs of HepG2 cells exposed to 1% CCL_4 alone or in presence of FLs or sylimarin.

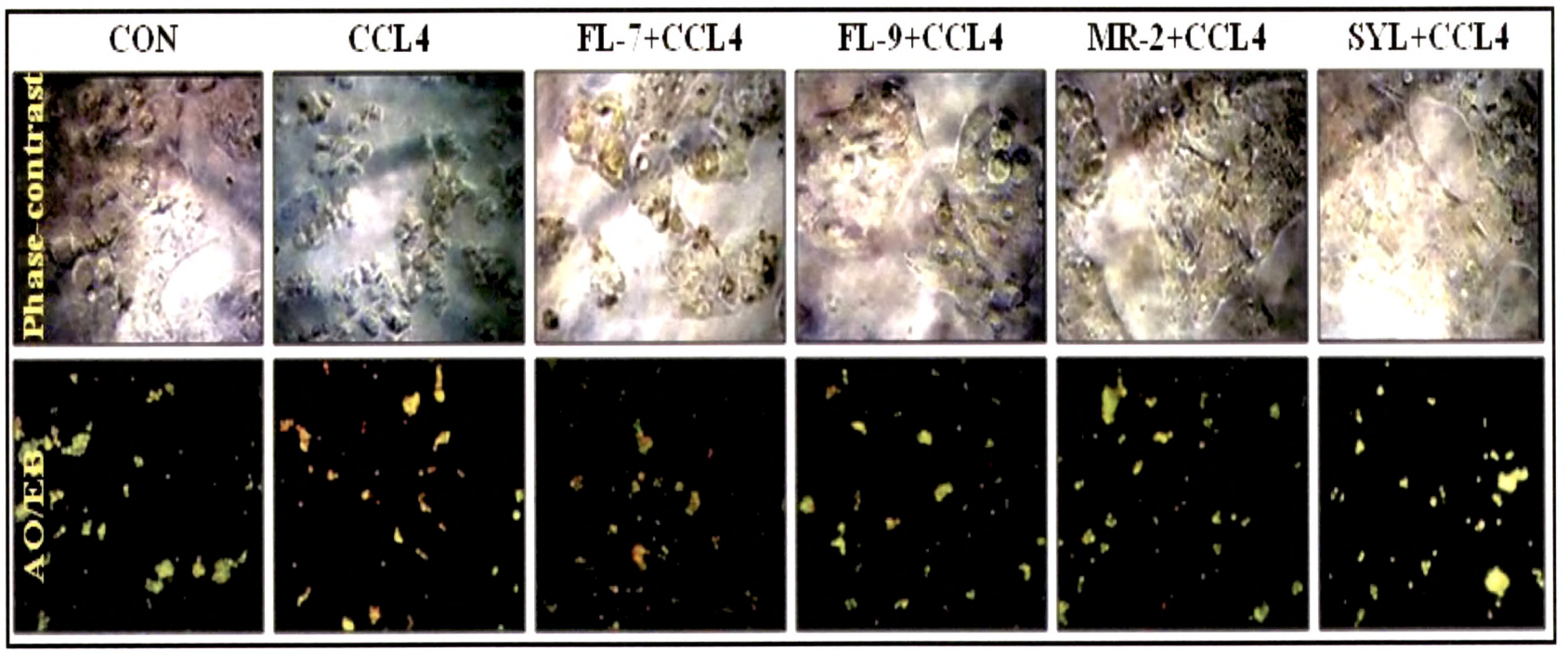

Figure 4.58 Phase contrast and AO/EB stained photomicrographs of HepG2 cells exposed to 1% CCL_4 alone or in presence of FSB7 or sylimarin.

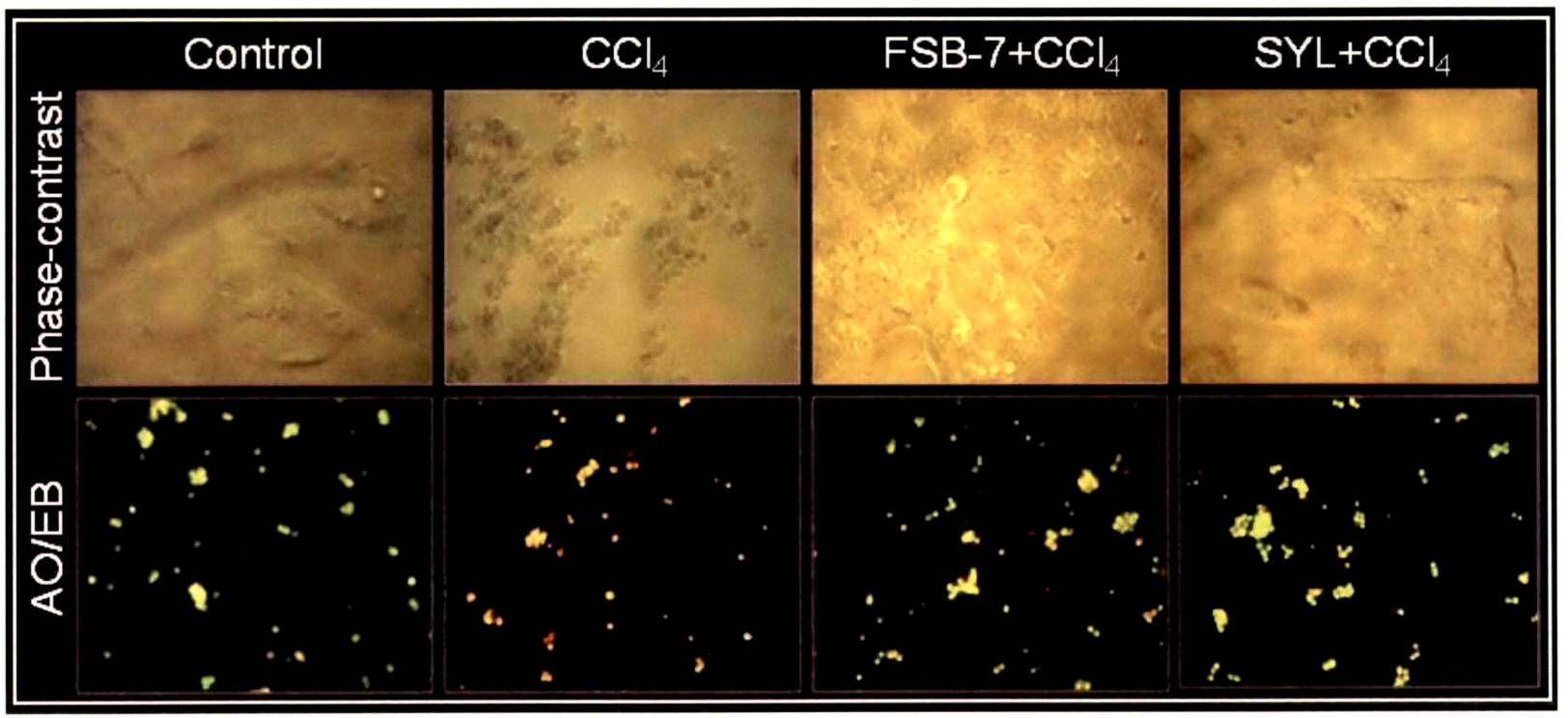

Figure 4.59 Phase contrast and AO/EB stained photomicrographs of HepG2 cells exposed to 1% CCL_4 alone or in presence of FRB7, MR-1 or sylimarin.

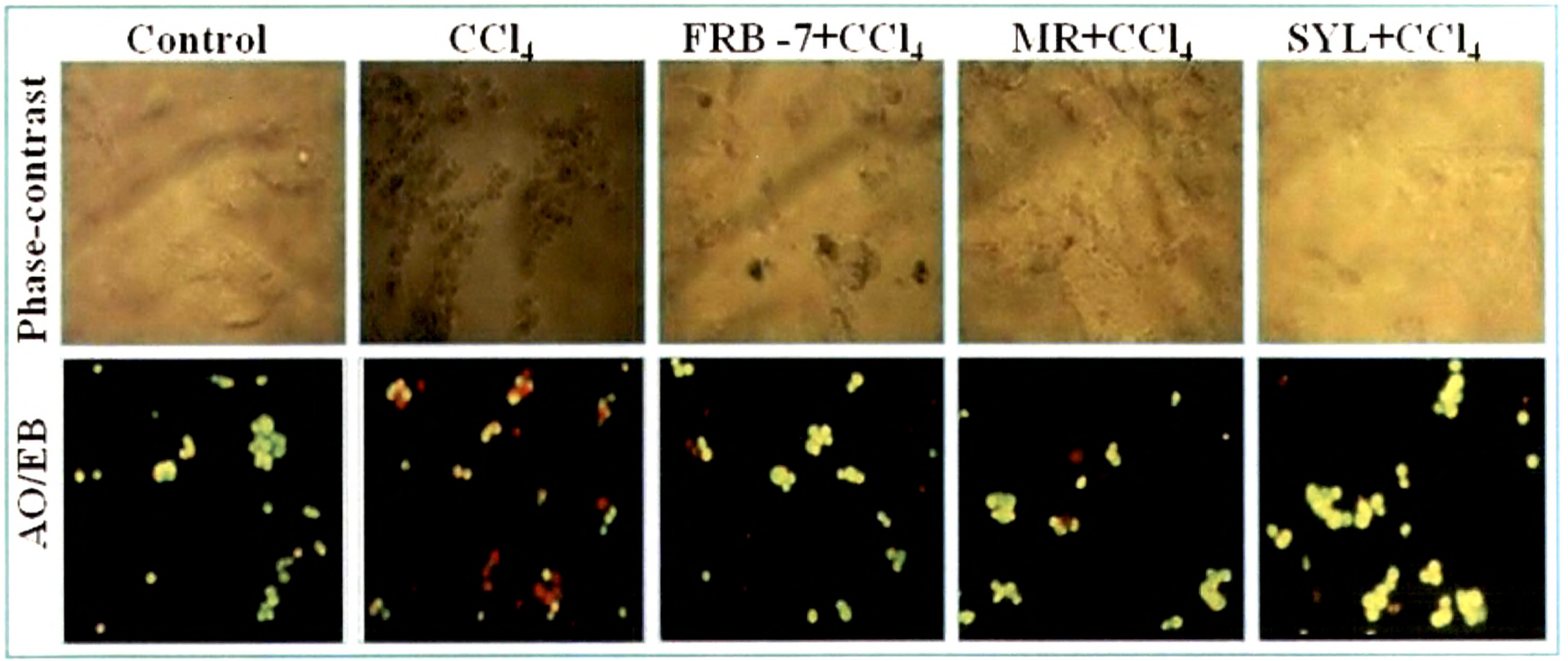

***In Vivo* Studies**

4.4.4 *In vivo* acute toxicity studies of *Feronia limonia*

The acute toxicity studies in rats were performed only in those samples of FLs, FSBs and FRBs which gave positive results for in vitro hepatoprotective activity.

4.4.4.a Acute toxicity studies of FLs

No mortality was recorded in animals that were orally administered up to 5000 mg/kg of FL-7, 2000 mg/kg FL-9 and 1000 mg/kg MR-2. There were also no adverse behavioral changes, diarrhoea, salivation or food aversion. There was no major change in the gross weight of animal.

4.4.4 b Acute toxicity studies of FSBs

No mortality was recorded in animals that were orally administered up to 5000 mg/kg of FSB-7. Here also there is no adverse behavioural changes, diarrhoea, salivation or food aversion.

4.4.4 c Acute toxicity studies of FRBs

No mortality was recorded in animals that were orally administered up to 5000 mg/kg of FRB-7 and 1000 mg/kg MR-1. There were also no adverse behavioral changes, diarrhoea, salivation or food aversion.

4.4.5 *In vivo* hepatic lipid peroxidation and antioxidants activity of *Feronia limonia*

One of the principal causes of CCl_4 induced liver injury is lipid peroxidation (LPO), induced and accelerated by free radical derivatives of CCl_4 (Maling et al., 1974). Free radicle scavenging enzymes, SOD and CAT and non-enzymatic antioxidants like GSH and AA are the first line of cellular defence against possible oxidative damage (Jayakumar et al., 2006; Lee et al., 2007; Gowri Shankar et al., 2008).SOD protects cells against free radicles by converting superoxide radicals into hydrogen peroxide, which is further metabolized by CAT to molecular oxygen and water, (Maheshwari et al., 2011) thus preventing oxidative damage. Changes in these parameters are hallmark of lipid peroxidation. Hence FLs, FSBs and FRBs are evaluatd for their antioxidant activity and for protection against CCl_4 induced lipid peroxidation.

4.4.5.a Antioxidant and lipid peroxidation studies of FLs

Elevated indices of LPO along with decreased content of GSH and AA and, activity levels of SOD and CAT was recorded in CCL_4 treated rats, which are consistence with the previous reports (Quan et al., 2011; Nitha et al., 2011).

FL-7 and FL-9 pre-treatment was able to prevent CCl_4 induced depletion of hepatic antioxidants, at higher dose (400mg/kg; 200mg/kg body weight) being most efficient and comparable to SYL + CCl_4 group. MR-2 (50 and 100 mg/kg body weight) recorded comparatively less significant level of mitigation as compared to SYL treated groups. Hepatic LPO levels were significantly high in CCl_4 treated groups. But, LPO level were similar in SYL, FL-7, FL-9 and MR-2 treated groups and comparable to control group (Table 4.15).

Table 4.15 Effect of FL-7, FL-9, MR-2 and sylimarin on hepatic antioxidants and lipid peroxidation during CCl_4 induced hepatotoxicity

Treatments	Superoxide dismutase (U/min/mg protein)	Catalase (U/min/mg protein)	Reduced glutathione (mg/g)	AA mg/g (mg/g)	LPO (nmol of MDA formed/mg Protein)
Control	63.00±2.88	34.16±0.92	6.45±0.27	4.12±0.06	2.83±0.02
CCl_4 control	26.09±1.15###	15.00±0.57###	2.31±0.02###	1.91±0.02###	5.81±0.06###
Silymarin+CCl_4	55.66±1.45***	31.00±0.59***	4.91±0.06**	3.68±0.06***	2.42±0.03***
FL-7 (200mg/kg)+CCL_4	44.33±1.20***	24.00±0.58**	3.91±0.02**	2.96±0.01***	3.15±0.02**
FL-7 (400mg/kg)+CCL_4	48.23±0.88***	26.00±0.31***	4.54±0.03***	2.65±0.28***	2.67±0.03***
FL-9 (100mg/kg)+CCL_4	46.35±0.88***	24.33±0.33**	4.13±0.07***	3.25±0.01***	2.67±0.02***
FL-9 (200mg/kg)+CCL_4	50.10±0.52***	27.00±0.59***	4.85±0.04***	3.72±0.02***	2.37±0.04***
MR-2 (50mg/kg)+CCL_4	47.33±3.05***	26.33±0.88***	4.89±0.09***	3.12±0.04***	2.9±0.06***
MR-2 (100mg/kg)+CCL_4	52.66±2.96***	29.33±1.20***	5.03±0.06***	3.74±0.13***	2.55±0.04***

4.4.5.b Antioxidant and lipid peroxidation studies of FSBs

In FSBs also significant decrement in status of hepatic enzymatic (SOD and CAT) and non-enzymatic (GSH and AA) antioxidants was recorded in CCl_4 treated rats. FSB-7 pre-treatment was able to prevent CCl_4 induced depletion of hepatic antioxidant. A dose of 400mg/kg body weight of FSB-7 was found to be most efficient and comparable to SYL + CCl_4 group. Hepatic LPO levels were significantly high in CCl_4 treated groups. But, LPO level were similar in SYL, FSB-7 treated groups and comparable to control group. Presently recorded minimum depletion of antioxidants and lowered LPO indices in FSB-7 treated animals is possibly due to high content of polyphenols and flavanoids that scavenge free radicals produced due to CCL_4 treatment. (Table 4.16)

Table 4.16 Effect of FSB-7 and sylimarin on hepatic antioxidants and lipid peroxidation during CCl_4 induced hepatotoxicity

Treatments	Superoxide Dismutase U/min/ mg/protein	Catalase U/min/ mg/protein	Reduced glutathione (mg/g)	Ascorbic acid (mg/g)	Lipid peroxidation Nmol of MDA formed/ mg/protein
Control	62.21±4.31	33.45± 1.56	7.00±0.45	4.21±0.25	2.77±0.39
CCl_4 control	25.53±1.88$^{###}$	16.14±1.99$^{###}$	2.45±0.21$^{###}$	1.89±0.22$^{###}$	5.67±0.21$^{###}$
Silymarin+ CCl_4	52.11±4.89***	31.11±2.11**	4.88±0.34***	3.54±0.17***	2.41±0.29***
FSB-7 (250mg/kg) + CCl_4	45.00±4.11***	22.33±0.53*	3.64±0.02*	2.86±0.04**	3.31±0.02**
FSB-7 (500mg/kg) + CCl_4	51.00±5.01***	27.00±0.35**	4.23±0.25***	3.23±0.05***	2.92±0.01***

Data expressed as mean± S.E.M. for n=6. Where, ###p<0.001 compared to control*p<0.05, **p<0,01 and ***p<0.001 compared to CCL_4

4.4.5.c Hepatic lipid peroxidation and antioxidant activity of Feronia limonia root bark

In FRBs too, CCl_4 treatment accounted for significant decrement in status of hepatic enzymatic (SOD and CAT) and non-enzymatic (GSH and AA) antioxidants. FRB-7 pre-treatment was able to prevent CCL_4 induced depletion of hepatic antioxidant with its higher dose (400mg/kg body weight) being most efficient and as effective as SYL + CCL_4 group. MR-1 (50 and 100 mg/kg body weight) recorded comparatively less

significant level of mitigation as compared to FRB-7 and SYL treated groups. Hepatic LPO levels were significantly high in CCL_4 treated groups. But, LPO level were similar in SYL, FRB-7 and MR-1 treated groups and comparable to control group (Table 4.17).

Table 4.17 Effects of FRB-7 and MR-1 on hepatic antioxidants and lipid peroxidation during CCl_4 induced hepatotoxicity

Treatments	Superoxide dismutase (U/min/mg protein)	Catalase (U/min/mg protein)	Reduced glutathione (mg/g)	AA (mg/g)	LPO (nmol of MDA formed/mg protein)
Control	63.00±4.33	34.16±11.00	6.45±0.27	4.12±0.22	2.83±0.40
CCL_4 control	26.00±2.45###	15.00±2.00###	2.31±0.26###	1.91±0.21###	5.81±0.23###
Silymarin+ CCL_4	53.66±5.09***	31.00±2.34**	4.91±0.44***	3.68±0.22***	2.42±0.33***
FRB-7 (200mg/kg)+CCL_4	53.70±4.43***	26.66±2.43*	4.22±0.40*	3.83±0.12***	2.48±0.23***
FRB-7 (400mg/kg)+CCl_4	60.70±4.09***	31.33±3.23***	5.02±0.45***	4.11±0.21***	2.34±0.17***
MR-1 (50mg/kg)+CCl_4	48.00±3.33**	24.00±1.56ns	3.71±0.22ns	2.76±0.23ns	2.23±0.13***
MR-1 (100mg/kg)+CCl_4	52.66±3.43***	27.66±1.78*	4.69±0.50**	3.14±0.24**	2.57±0.14***

Data expressed as mean± S.E.M. for n=6. Where, ###p<0.001 compared to control and *p<0.05, **p<0, 01 and ***p<0.001 compared to CCL_4 control

4.4.6 *In vivo* CCl_4 induced hepatotoxicity of *Feronia limonia*

CCl_4 induced hepatotoxicity is initiated in the form of intracellular damage to the endoplasmic reticulum and progresses by affecting cellular metabolic enzymes (Recknagel et al., 1989). The toxic metabolite CCl_3^* radical is produced which is further converted to trichloromethyl peroxy radical by cytochrome P450 2E1 enzyme. This radical binds covalently to the macromolecules and causes peroxidative degradation of cellular membrane leading to the necrosis of hepatocytes (Lima et al., 2007; Shyu et al., 2008; Hsu et al., 2009). Higher degree of lipid peroxidation in the hepatic tissue of CCL_4 treated rats is a hallmark of hepatotoxicity. Also, it has been inversely correlated with the tissue antioxidant status (Maheshwari et al., 2011).

4.4.6 a In vivo: CCl_4 induced hepatotoxicity of FLs

CCl_4 treated group recorded significantly elevated level of SGOT, SGPT (AST, ALT) ALP and total bilirubin whereas the total protein content in plasma significantly reduced. However, FL-7, FL-9 and MR-2 treated groups prevented CCl_4 induced elevation in plasma markers of hepatic damage and prevented CCl_4 induced decrement in plasma protein. Higher dose of FL-7 (400mg/kg body weight) and FL-9 (200mg/kg body weight) were the most efficient in mitigating CCl_4 induced hepatotoxicity. MR-2 (50 and 100 mg/kg body weight) also recorded similar set of changes but the plasma AST level recorded non- significant decrement with both the dose (Table 4.17).

Table 4.18 Effects of FL-7, FL-9, MR-2 and sylimarin on plasma levels of hepatic injury markers during CCl_4 induced hepatotoxicity.

Treatments	Alanine Transaminase (U/L)	Asparate Transaminase (U/L)	Alkaline phosphate (U/L)	Total protein (g%)	Bilirubin (g%)
Control	48.33±1.49	85.33±1.07	1.74±0.012	7.89±0.028	1.38±0.015
CCl_4 control	145.33±2.86###	330.16±5.72###	3.57±0.022###	4.86±0.054###	3.92±0.455###
Silymarin+CCl_4	50.83±1.87***	95.83±1.38***	1.85±0.015**	7.52±0.031***	1.54±0.020***
FL-7 (200mg/kg)+CCL_4	67.832.26***	131.33±4.06**	2.38±0.044**	6.35±0.027**	2.22±0.019*
FL-7 (400mg/kg)+CCL_4	58.5±3.00***	112.00±2.06***	2.21±0.018**	6.86±0.079***	1.94±0.012**
FL-9 (100mg/kg)+CCL_4	59.66±4.14***	111.83±2.56**	2.10±0.044**	6.87±0.029**	1.84±0.028***
FL-9 (200mg/kg)+CCL_4	52.00±3.81***	99.16±4.69***	1.91±0.025***	7.58±0.037***	1.48±0.020***
MR-2 (50mg/kg)+CCL_4	66.33±3.35***	119±1.50***	2.47±0.16**	7.02±0.03**	1.92±0.01***
MR-2 (100mg/kg)+CCL_4	53.66±2.49***	97.33±3.43***	1.98±0.01***	7.33±0.06***	1.64±0.04***

Data expressed as mean± S.E.M. for n=6. Where, ###p<0.001 compared to control and *p<0.05, **p<0.01 and ***p<0.001 compared to CCL_4.

4.4.6.b In vivo CCl_4 induced hepatotoxicity of FSBs

CCL_4 induced severe hepatocyte membrane damage or necrosis results in the leakage of marker enzymes of liver function in to the plasma and hence, elevations in plasma levels of AST, ALT, ALP, bilirubin and total protein are indicator of hepatotoxicity

(Palinivel et al., 2008). Presently recorded elevated levels of AST, ALT, ALP, bilirubin and total protein in the CCL_4 treated rats are in accordance with previous reports (Domitrović et al., 2009; Jodynis-Liebert et al., 2009). The restoration of these parameters to near control levels in CCl_4+FSB-7 treated group indicates at the ability of FSB-7 in preventing leakage of intra cellular enzymes and bilirubin and stands well correlated with histopathological evaluations. It is assumed that FSB-7 imparts hepatoprotection against free radicals induced oxidative damage and stabilizes the hepatic cell membrane against further degradation (Table 4.19).

Table 4.19 Effects of FSB-7 and sylimarin on plasma levels of hepatic injury markers during CCl_4 induced hepatotoxicity.

Treatments	Alanine transaminase (U/L)	Aspartate transaminase (U/l)	Alkaline phosphatase (U/l)	Total protein (g%)	Bilirubin (g%)
Control	46.11±2.99	84.66±9.00	1.69±0.13	8.00±0.84	1.40±0.22
CCL_4	140.41±4.23###	280.16±12.41###	3.78±0.31##	4.54±0.94###	3.88±0.42###
Silymarin+ CCL_4	52.41±3.00***	92.11±12.56***	1.45±0.23*	7.00±0.71***	1.51±0.21***
FSB-7 (200mg/kg)+CCL_4	71.66±2.59**	142.16±13.04**	2.52±0.10*	6.26±0.02**	2.50±0.25**
FSB-7 (400mg/kg)+CCL_4	62.83±4.20***	121.16±11.76***	2.25±0.21*	6.55±0.03**	2.07±0.02**

Data expressed as mean± S.E.M. for n=6. Where, ###p<0.001 compared to control and *p<0.05, **p<0.01 and ***p<0.001 compared to CCL_4.

4.4.6.c In vivo CCl_4 induced hepatotoxicity of FSBs

In FRBs, CCl_4 treated group shows significantly higher level of plasma AST, ALT, ALP and total bilirubin whereas, the total protein content was significantly reduced. However, FRB-7 and MR-1 treated groups prevented CCl_4 induced elevation in plasma markers of hepatic damage and prevented CCl_4 induced decrement in plasma protein. Higher dose of FRB-7 (400mg/kg body weight) was the most efficient in mitigating CCl_4 induced hepatotoxicity. MR-1(50 and 100 mg/kg body weight) also recorded similar set of changes but the plasma AST level recorded a non- significant decrement with these doses (Table 4.20).

Table 4.20Effects of FRB-7 and MR-1 on plasma levels of hepatic injury markers during CCl_4 induced hepatotoxicity

Treatments	Alanine Transaminase (U/L)	Asparate Transaminase (U/I)	Alkaline Phosphatise (U/L)	Bilirubin (g%)	Total protein (g%)
Control	48.33±3.23	85.33±11.00	1.74±0.13	1.38±0.22	7.89±0.84
CCL_4	145.33±5.43###	330.16±15.91###	3.57±0.31##	3.92±0.41###	4.86±0.94###
Silymarin+ CCL_4	50.83±3.42***	95.83±13.00***	1.85±0.29*	1.54±0.21***	7.52±0.71***
FRB-7 (200mg/kg)+CCL_4	62.50±4.00***	145.33±10.00***	2.00±0.45*	2.01±0.40**	6.84±0.91**
FRB-7 (400mg/kg)+CCL_4	46.33±3.72***	93.50±8.76***	1.82±0.34*	1.41±0.38***	7.50±0.73***
MR-1 (50mg/kg)+CCL_4	67.33±3.39***	133.50±8.99***	2.46±0.34ns	2.22±0.39ns	6.43±0.65*
MR-1 (100mg/kg)+CCL_4	61.66±3.11***	118.50±8.00***	2.27±0.31*	2.02±0.33*	6.65±0.81**

Data expressed as mean± S.E.M. for n=6. Where, ###p<0.001 compared to control and *p<0.05, **p<0,01 and ***p<0.001 compared to CCL_4 control.

4.4.7 In vivo: Histopathology of Liver

4.4.7.a Morphological and histopathological changes in liver after treatment with FLs

Microscopic evaluation of liver sections of control rats depicted unaltered cellular architecture with distinct hepatic cells, sinusoidal spaces, and a central vein.

Results of histopathology shows that the histo- architecture of liver was completely damaged in CCl_4 treated group. HXE stained section of CCl_4 treated rats, were characterized by loss of cellular boundries, infiltration of inflammatory cells, cytoplasmic vaculation, fatty change, centrilobular necrosis, and severe collagen deposition.

Picro-sirus red staining also revealed massive collagen deposition due to excessive formations of scars and connective tissue in tissue sections of CCl_4 group. These cellular changes were greatly reduced in FL-7, FL-9 and MR-2 treated group with higher dose of FL-7; FL-9 and MR-2 (400; 200 and 100 mg/kg body weight) recording mild necrosis and healthy hepatocytes that were comparable to control and SYL treated group (Figure 4.60).

Figure 4.60 Morphological, haematoxyline-eosin and picro-sirus stained photomicrographs of rat liver treated with CCL_4 alone or in presence of FSB-7 or sylimarin.

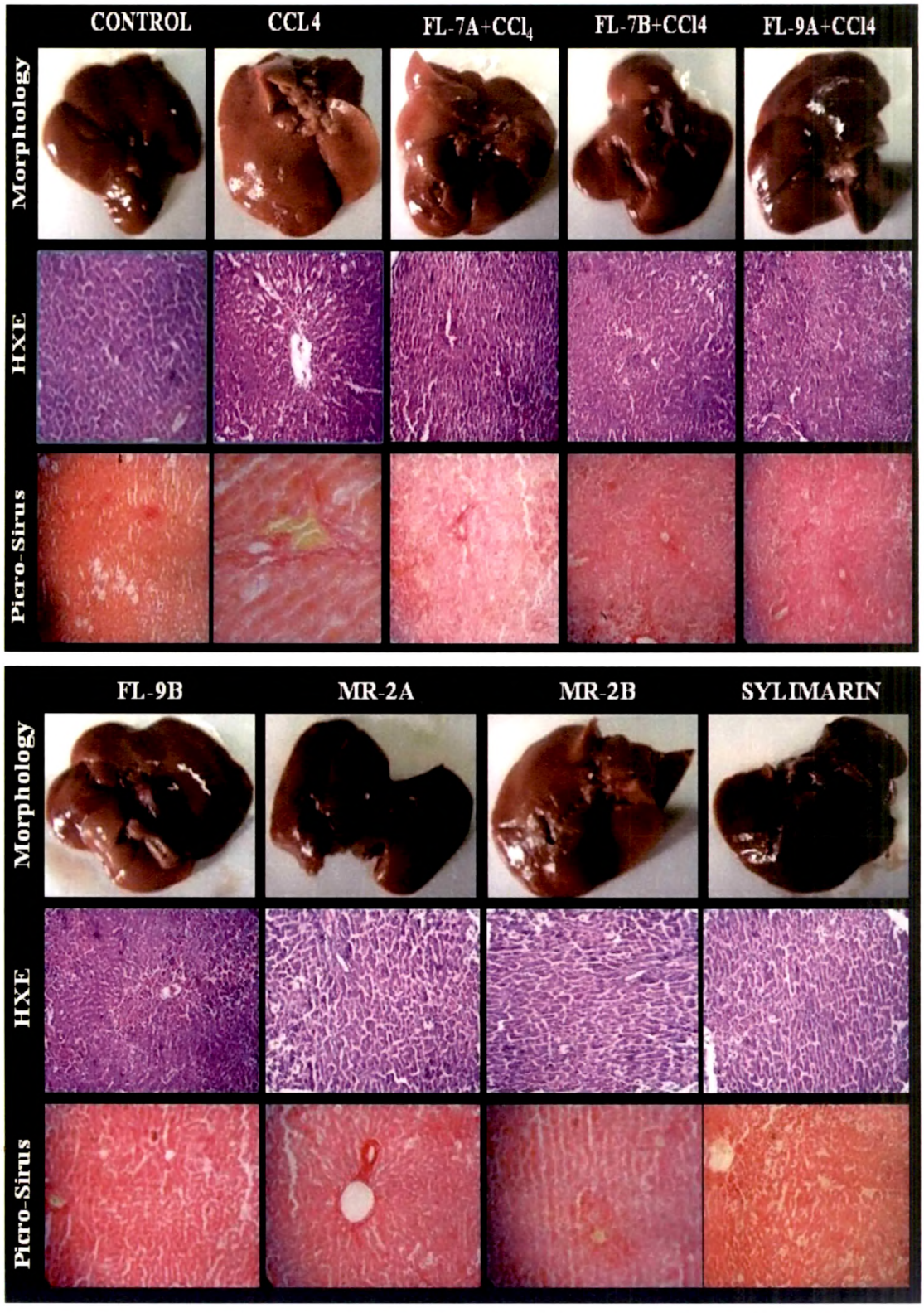

4.4.7.b Morphological and histopathological changes in liver after treatment with FSBs

In CCl_4 treated group, hepatocyte vaculation, centrilobular necrosis and nuclear condensation were evident in HXE stained liver section. Liver sections stained with picro-sirus red revealed massive collagen deposition due to excessive formations of scars and connective tissue in CCl_4 group. These cellular changes were greatly reduced in FSB-7 treated group with higher dose (400 mg/kg body weight) recording mild necrosis and relatively healthy hepatocytes that were comparable to the control and SYL treated groups (Figure 4.61).

Figure 4.61 Morphological, haematoxyline-eosin and picro-sirus stained photomicrographs of rat liver treated with CCL_4 alone or in presence of FSB-7 or sylimarin.

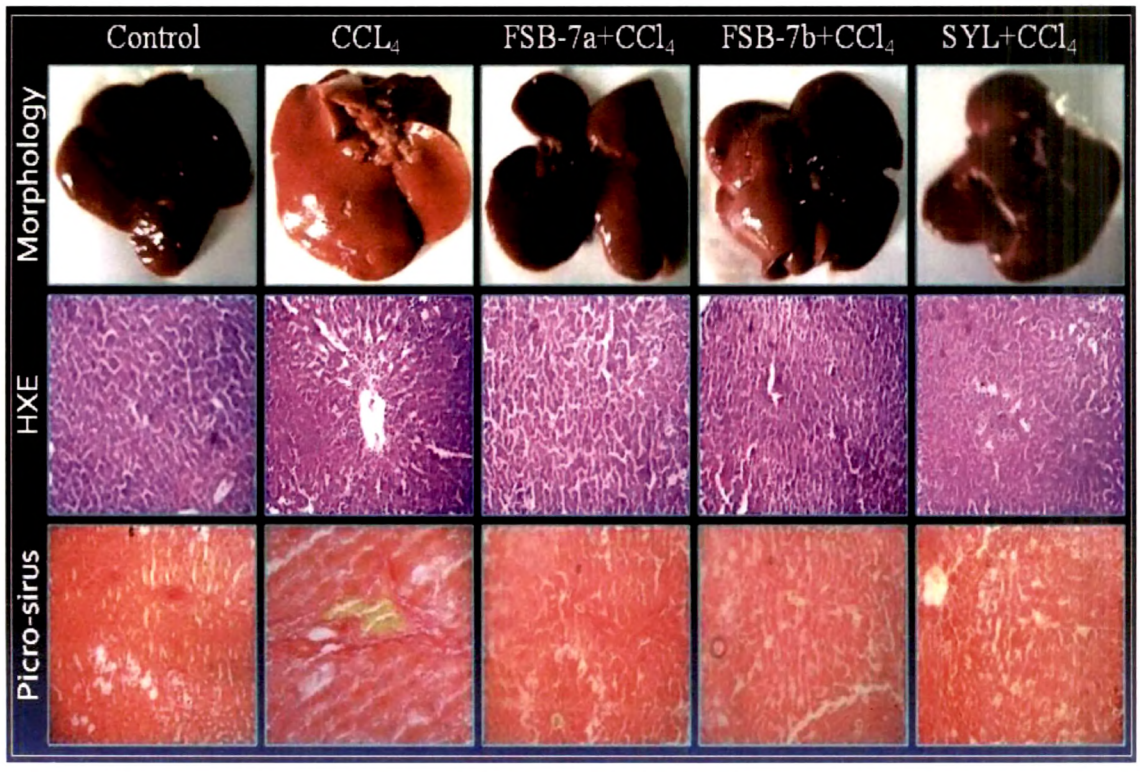

4.4.7 c Morphological and histopathological changes in liver after treatment with FRBs

Histopathological evaluation of liver of CCL_4 treated rats showed fat leaden hepatocytes, with loss of cellular boundary and extensive necrosis. There was broad infiltration of lymphocytes and kupffer cells in the centrilobular regions of liver. These results were in accordance with previous studies on histopathological alterations induced by CCL_4 treatment (Hsu et al., 2009; Tung et al., 2009). Further, studies have reported CCL_4 induced hepatic fibrosis (collagen deposition) in rats (Liu

et al., 2006; Shyu et al., 2008) and the same was observed in our study in the tissue section stained with picro sirus red. FRB-7 and MR-1 pre-treated rats showed relatively healthy hepatocytes with minimal necrosis or fibrosis. These observations provide visual evidence of hepatoprotective activity of FRB-7 and MR-1 (Figure 4.63).

Figure 4.62 Effect of FRB-7, MR and sylimarin on hepatic collagen deposition (picro-sirus red staining) during CCL_4 induced hepatotoxicity.

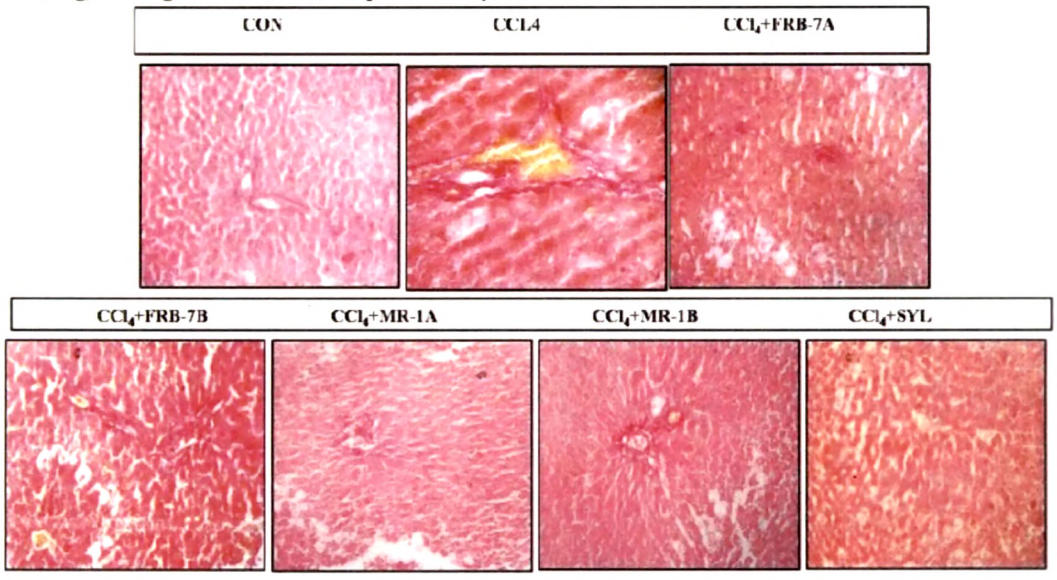

Figure 4.63 Effect of FRB-7, MR and sylimarin on hepatic histopathological alterations during CCL_4 induced hepatotoxicity.